



저작자표시-비영리-변경금지 2.0 대한민국

이용자는 아래의 조건을 따르는 경우에 한하여 자유롭게

- 이 저작물을 복제, 배포, 전송, 전시, 공연 및 방송할 수 있습니다.

다음과 같은 조건을 따라야 합니다:



저작자표시. 귀하는 원저작자를 표시하여야 합니다.



비영리. 귀하는 이 저작물을 영리 목적으로 이용할 수 없습니다.



변경금지. 귀하는 이 저작물을 개작, 변형 또는 가공할 수 없습니다.

- 귀하는, 이 저작물의 재이용이나 배포의 경우, 이 저작물에 적용된 이용허락조건을 명확하게 나타내어야 합니다.
- 저작권자로부터 별도의 허가를 받으면 이러한 조건들은 적용되지 않습니다.

저작권법에 따른 이용자의 권리는 위의 내용에 의하여 영향을 받지 않습니다.

이것은 [이용허락규약\(Legal Code\)](#)을 이해하기 쉽게 요약한 것입니다.

[Disclaimer](#)

**Role of type I interferon signaling  
in kainic acid-induced seizure model**

**Jeong-Hwa Ma**

**The Graduate School  
Yonsei University  
Department of Medical Science**

# **Role of type I interferon signaling in kainic acid-induced seizure model**

**A Master's Thesis Submitted  
to the Department of Medical Science  
and the Graduate School of Yonsei University  
in partial fulfillment of the  
requirements for the degree of  
Master's of Medical Science**

**Jeong-Hwa Ma**

**June 2024**

This certifies that the Master's Thesis  
of MA JEONGHWA is approved

Thesis Supervisor Jun Young Seo

Thesis Committee Member Ji Won Um

Thesis Committee Member Je Wook Yu

The Graduate School  
Yonsei University

June 2024

## ACKNOWLEDGEMENTS

As I complete my degree program, I would like to take this opportunity to express my heartfelt gratitude to the people who have helped me reach this point.

First and foremost, I would like to acknowledge and give my warmest thanks to my supervisor, Je-Wook Yu, for giving me the opportunity to conduct research and guiding me through my academic journey. Your dedication and support have been instrumental in helping me find direction and move forward. I am also sincerely grateful to Professor Jun-Yong Seo and Ji Won Um for their valuable time and effort in reviewing my thesis. Your guidance has been crucial in successfully completing my degree.

I would also like to thank my lab members, who have been my companions through this long journey of three years: Dr. Shim, In-Hwa Hwang, Sung-Hyun Yoon, Jun-Cheol Eo, Bo-keum Choi, Byeong-Jun Chae, Sae-Young Kim, Chang-Jun Lee, Kyung-Seo Lee, Jae-Eun Shin, Ha-Rin Bae, and Yun-Jeong Yang. Thanks to all of you, I was able to endure the challenging moments and overcome them with resilience.

Lastly, I express my deepest gratitude and love to my family, who have believed in me and supported me throughout my degree program. Your unwavering support and encouragement have enabled me to complete my degree.

As I now step forward towards a new path, I feel a mix of fear and excitement. However, I will confidently take each step, keeping in mind the valuable lessons learned during my degree program. I promise to become a better person and once again extend my heartfelt thanks to all those who have helped me along the way.

Sincerely,  
Jeong-Hwa Ma

## TABLE OF CONTENTS

LIST OF FIGURES .....	iii
LIST OF TABLES .....	iv
ABSTRACT IN ENGLISH .....	v
1. INTRODUCTION .....	1
2. MATERIAL AND METHODS .....	4
2.1. Mice .....	4
2.2. Reagents and antibodies .....	4
2.3. Kainic acid-induced seizures .....	4
2.4. Immunohistochemistry .....	5
2.5. TUNEL assay .....	5
2.6. Nissl staining .....	6
2.7. Quantitative real-time PCR .....	6
2.8. Flow cytometry .....	8
2.9. Western blot and ELISA .....	8
2.10. Statistical analysis .....	8
3. RESULTS .....	10
3.1. Kainic acid injection induces neural hyperactivity and the development of seizures	10
3.2. Microglia are activated in the acute phase of seizures .....	13
3.3. Kainic acid injection induces neuronal death and gliosis in the late phase of seizures	17
3.4. Type I interferon signaling is activated during the late phase of seizures in the hippocampus .....	23
3.5. Kainic acid-induced seizures are attenuated in <i>Ifnar1</i> knockout mice .....	26

3.6. The absence of type I interferon signaling reduces neuronal activity and microgliosis in the acute phase of seizures .....	28
3.7. There is no significant difference in neuronal death and gliosis between WT and <i>Ifnar1</i> knockout mice during the late phase of seizures .....	31
4. DISCUSSION .....	36
5. CONCLUSION .....	38
REFERENCES .....	39
ABSTRACT IN KOREAN .....	44

## LIST OF FIGURES

<Fig 1> Kainic acid-induced acute seizure development in mice .....	11
<Fig 2> Increased expression pattern of c-FOS in the hippocampus and cortex following kainic acid-induced seizures .....	12
<Fig 3> Microglia activation in the acute phase of seizures .....	14
<Fig 4> Neuronal death in the late phase of seizures .....	18
<Fig 5> Gliosis in the late phase of seizures .....	19
<Fig 6> Glia activation in the late phase of seizures .....	21
<Fig 7> Microglia proliferation and immune cell infiltration in the late phase of seizures .....	22
<Fig 8> Lack of type I interferon signaling in the hippocampus during seizures .....	24
<Fig 9> Type I interferon signaling activation in the hippocampus after seizures .....	25
<Fig 10> Decreased seizure severity in <i>Ifnar1</i> knockout mice .....	27
<Fig 11> Decreased c-FOS expression with loss of type I interferon signaling following kainic acid-induced seizures .....	29
<Fig 12> Altered microglial activation due to loss of type I interferon signaling following kainic acid-induced seizures .....	30
<Fig 13> Absence of neuronal death in the late phase of seizures in both WT and <i>Ifnar1</i> <sup>-/-</sup> mice .....	32
<Fig 14> Comparable gliosis levels in WT and <i>Ifnar1</i> <sup>-/-</sup> mice post seizures .....	33
<Fig 15> No notable difference in microglia morphology between WT and <i>Ifnar1</i> <sup>-/-</sup> mice in the late phase of seizures .....	34
<Fig 16> Suggested explanations for reduced seizure severity in <i>Ifnar1</i> <sup>-/-</sup> mice .....	35

## LIST OF TABLES

<Table 1> Primer sequence for PCR .....	7
---	---

## ABSTRACT

### **Role of type I interferon signaling in kainic acid-induced seizure model**

Epilepsy is a chronic neurological disorder characterized by repeated seizures resulting from excessive neuronal activity. Despite there being a variety of anti-epileptic drugs targeting neuronal excitability, almost one-third of patients are refractory to these treatments, underscoring the need for a deeper understanding of the pathological events and molecular changes during epileptogenesis. Type I interferon (IFN) signaling has been suggested as a significant factor in brain development and homeostasis, and its dysregulation has also been related to various central nervous system (CNS) diseases, including Alzheimer's disease. According to a recent study, microglia in kainic acid-induced seizures show an increase in interferon beta responsiveness. However, the specific role of type I IFN signaling in seizures remains unclear. Therefore, in this study, we aimed to elucidate the function of type I IFN signaling in seizures using kainic acid to induce seizures in mice. We observed upregulation of interferon beta and interferon-stimulated genes in the hippocampus of these mice, indicating the involvement of type I IFN signaling in seizures. For further examination, we induced seizures in C57BL/6 wild-type mice and *Ifnar1* knockout mice, which are type I IFN receptor-deficient mice, to compare the severity of seizures and subsequent events. Interestingly, *Ifnar1* knockout mice exhibited attenuated seizure severity and higher mortality during the onset of seizures. Furthermore, *Ifnar1* knockout mice showed decreased neuronal activity and different aspects of microgliosis during the acute phase of seizures. However, interferon signaling did not significantly impact neuronal death and gliosis in the late phase of seizures. These data imply that the presence of type I IFN signaling is essential for CNS maintenance and that its absence can affect microglial function and neuronal activation. These results suggest the potential therapeutic utility of type I IFNs as a target for treating seizures and epilepsy.

---

Key words : epilepsy, seizure, interferon, microglia, neuron

## 1. Introduction

Epilepsy is a chronic neurological disorder characterized by repeated seizures, affecting more than 65 million people worldwide<sup>1,2</sup>. It can arise from genetic mutations or a combination of genetic predisposition and environmental factors such as traumatic brain injury, stroke, or neurological infections<sup>3</sup>. Under normal conditions of neural homeostasis, neuronal activity is tightly regulated through various mechanisms<sup>4,5</sup>. Within individual neurons, regulation occurs via voltage-gated ion channels and G-protein-coupled receptors (GPCRs)<sup>4</sup>. Additionally, the interactions between neurons play a crucial role, particularly through the release of neurotransmitters at the synapse. Excitatory neurotransmitters like glutamate induce post-synaptic neuron excitation, whereas inhibitory neurotransmitters like GABA inhibit this excitation<sup>5</sup>. However, disruptions in the balance of excitation and inhibition of neurons—due to abnormal ion channel activity, synaptic dysfunction, neurotransmitter release imbalance, or enhanced neuronal network connectivity—can lead to seizures and epilepsy<sup>6</sup>. Therefore, current anti-epileptic drugs (AEDs) have traditionally targeted neuronal mechanisms of excitability by interacting with ion channels or neurotransmitter receptors. Despite there being a variety of available AEDs, almost one-third of patients are refractory to these treatments, highlighting gaps in our understanding of epileptogenesis—the gradual process by which a normal brain develops epilepsy<sup>7,8</sup>. Thus, a deeper understanding of the pathological processes and molecular alterations during epileptogenesis is crucial for developing more efficacious treatments for epilepsy patients.

Glia are non-neuronal cells found in the central and peripheral nervous systems<sup>9</sup>. Several studies have reported that glial cells, especially microglia functioning as immune cells and astrocytes providing metabolic support to neurons, contribute to epileptic conditions<sup>10-22</sup>. Extensive activation of these cells has been observed during the latent period of epilepsy<sup>10-16</sup>. Microglia, in particular, have dual roles in epilepsy pathogenesis<sup>17,18</sup>. They can act protectively by surveilling the brain microenvironment, detecting abnormal neuronal hyperexcitability, and stabilizing neurons through interactions<sup>19-21</sup>. However, microglia can also exacerbate epilepsy by increasing neuronal hyperexcitability, causing neuronal death, triggering aberrant neurogenesis, and promoting neuroinflammation<sup>10-12,22</sup>. This highlights the complexity of

microglial functions, which can vary depending on the brain microenvironment and the stage of epilepsy.

Type I interferons (IFNs) are crucial cytokines involved in antiviral response, inflammation, and immunoregulation<sup>23-25</sup>. Upon binding to their receptor IFN- $\alpha/\beta$  receptor (IFNAR), type I IFNs initiate signaling cascades involving JAK1/TYK2 activation, which includes both the canonical JAK-STAT pathway and non-canonical pathways like phosphoinositide 3-kinase (PI3K)/ mammalian target of rapamycin (mTOR) pathways<sup>26</sup>. These pathways lead to the up-regulation of interferon-stimulated genes (ISGs), proinflammatory cytokines, and chemokines<sup>23,27</sup>. In the central nervous system (CNS), microglia are the primary sources of type I IFN production, notably IFN- $\beta$ , which are continuously present in the CNS at low concentrations<sup>28</sup>. Furthermore, IFNAR1 is expressed in most cell types within the brain, including excitatory and inhibitory neurons, microglia, astrocytes, and endothelial cells. Several studies have recently proposed that type I IFNs might contribute to the development and maintenance of the CNS<sup>29-33</sup>. Neurons rely on type I IFN signaling during development, and this signaling is also crucial for synaptic plasticity and cognitive function, specifically mediated by astrocytes<sup>29,32</sup>. Microglia, on the other hand, utilize type I IFN signaling for their phagocytic activities<sup>33</sup>. Furthermore, dysregulation of type I IFN signaling has been associated to various CNS diseases, such as Alzheimer's disease, Parkinson's disease, Down's syndrome, and traumatic brain injury<sup>29,34-42</sup>. For example, abnormal type I IFN signaling in microglia and neural cells promotes synapse loss and plaque accumulation in Alzheimer's disease, while an absence of neuronal type I IFN signaling is linked to brain Lewy body accumulation, leading to Parkinson's disease-like dementia<sup>41,42</sup>. Therefore, the precise regulation of type I IFN signaling might be significant for maintaining CNS homeostasis.

A recent study has revealed that type I IFN signaling is upregulated in seizure-induced microglia<sup>43</sup>. Additionally, several clinical reports have demonstrated that spontaneous seizures can occur during alpha interferon therapy<sup>44,45</sup>. Furthermore, research has shown that Poly I:C injection into the brain decreased seizure severity in vivo, and IFN- $\beta$  treatment reduced synaptic excitability ex vivo<sup>46</sup>. These findings collectively suggest that type I IFNs might be involved in the initiation and progression of seizures. However, the specific role of type I IFN signaling in seizures and its underlying mechanisms remain elusive. In our study, using *Ifnar1* knockout mice, we observed reduced seizure severity and different aspects of microgliosis during the acute phase

of seizures in these knockout mice compared to wild-type mice under kainic acid-induced seizure conditions. This observation suggests that a deficiency in type I IFN signaling may contribute to altered CNS conditions during development, or that the interruption of type I IFN signaling may affect microglia and neuronal activity during seizures. These results highlight the importance of type I IFN signaling in the CNS and suggest the potential of type I IFNs as a therapeutic target for mitigating seizures and epilepsy.

## 2. Materials and methods

### 2.1. Mice

C57BL/6 mice were either bred in-house or acquired from Orient Bio (Seongnam, Korea). *Ifnar1<sup>-/-</sup>* mice (B6.129S2-*Ifnar1*<sup>tm1Agt/Mmjax</sup>) (The Jackson Laboratory, Bar Harbor, ME, USA) were kindly provided by Dr. Sung Jae Shin (Yonsei University, Korea). All mice were maintained under specific pathogen-free conditions, and 8- to 12-week-old male mice were used for the experiments. All experimental procedures were conducted in accordance with the approved guidelines of the Institutional Ethical Committee, Yonsei University College of Medicine.

### 2.2. Reagents and antibodies

Kainic acid was purchased from R&D (Minneapolis, MN, USA) for mice injection. For immunohistochemistry, anti-IBA1 (Wako, Monzo, Italy), anti-GFAP (Invitrogen, Waltham, MA, USA), anti-c-FOS and anti-NeuN (Cell Signaling Technology, Boston, MA, USA) antibodies were used. Regarding the antibodies used for flow cytometry, anti-CD45-APC-cy7 antibody was purchased from Biolegend (San Diego, CA, USA) and anti-CD11b-PE antibody was obtained from Invitrogen. For western blot, rabbit anti-STAT1, mouse anti-IRF9, and mouse anti- $\beta$ -actin antibodies were purchased from Cell Signaling Technology. The mouse anti-viperin antibody was kindly gifted by Dr. Jun-Young Seo (Yonsei University, Korea).

### 2.3. Kainic acid-induced seizures

To induce seizures, the mice received intraperitoneal injections of kainic acid (20-25 mg/kg) dissolved in saline. Seizure behavior was monitored for 2 hours at 10-minute intervals using the modified Racine scale<sup>47</sup>: (0) no response; (1) freezing behavior; (2) continuous head bobbing; (3) rearing; (4) continuous rearing and falling; (5) loss of posture and generalized convulsive activity; (6) death. Mice that reached stage 3 or above were used for the experiments. Control mice received saline injections and exhibited no abnormal behavior.

## 2.4. Immunohistochemistry

Mice were deeply anesthetized with isoflurane (5% in O<sub>2</sub>) and transcardially perfused with 20 ml PBS followed by 10 ml 4% paraformaldehyde (PFA). Dissected brains were post-fixed in 4% PFA for 48 hours and then cryoprotected in 30% sucrose for 72 hours at 4°C. Brains were subsequently cut into 40- $\mu$ m frozen sections with Leica CM1860 cryostat. The sections were blocked and permeabilized in blocking solution containing 4% BSA and 0.3% Triton X-100 at room temperature for 60 minutes. Subsequently, sections were incubated with anti-IBA1 (1:500), anti-GFAP (1:500), anti-c-FOS (1:500), or anti-NeuN (1:500) antibodies diluted in blocking solution for 24-48 hours at 4°C. Sections were washed with PBST several times, then incubated with Cy3 or Alexa Fluor 488-conjugated secondary antibodies (Invitrogen) at room temperature for 1-2 hours in the dark. After washes, nuclei were visualized with DAPI, and coverslips were coated with antifade (Thermo Fisher Scientific, Waltham, MA, US). Z-stack images were acquired at 0.75-1  $\mu$ m intervals over a 30  $\mu$ m Z-range using a confocal microscopy (LSM780 or LSM980; Carl Zeiss) with 20 x or 40 x magnification. Z-stack images were converted into single-plane maximal intensity projection using ZenBlue (Carl Zeiss). ImageJ (NIH) was used to measure mean fluorescence intensity (MFI) and count the number of cells. For microglia-neuronal soma interaction analyses, IBA1 and NeuN co-staining images were analyzed using ImageJ. Briefly, channels were split into single channels, and 20-30 region of interests (ROIs) were drawn around each neuronal soma. Subsequently, the ROIs were overlaid onto the IBA1 channel, and the IBA1 area within each ROI was measured. For 3D image analyses, z-stack images were reconstructed using Imaris software (BitPlane). The soma volume of microglia was calculated using the Surface feature, and the Filament feature was used to calculate the number of branch points and terminal points, as well as for Sholl analysis. For each image, 3-4 microglia were randomly chosen, and the average value was calculated.

## 2.5. TUNEL assay

The terminal deoxynucleotidyl transferase (TdT)-mediated dUTP biotin nick end-labeling (TUNEL) assay was performed using the in situ cell death detection kit (Roche, Basel, Swiss). According to manufacturer's instructions, brain sections were fixed with 4% PFA at room

temperature for 20 minutes, washed with PBS, and incubated in permeabilization solution containing 0.1% Triton X-100 in 0.1% sodium citrate for 2 minutes on ice. The sections then rinsed with PBS and incubated with TUNEL reaction mixture for 90 minutes at 37°C in a humidified atmosphere in the dark. Subsequently, the sections were rinsed with PBS, stained with DAPI, and mounted in antifade. Confocal microscopy was used for the image with 20 x magnification. The number of TUNEL-positive cells was manually counted and the ratio of the TUNEL-positive cells to total nuclei (DAPI) was calculated.

## 2.6. Nissl staining

Tissue sections were incubated in a defatting solution (50:50 chloroform and 100% ethanol) for at least one hour to remove lipids. The sections were then rehydrated in a decreasing ethanol gradient, stained with 0.1% cresyl violet (Sigma-Aldrich, St. Louis, MO, USA) for 3 minutes, and quickly rinsed with distilled water. Following rinsing, the sections were differentiated in 95% ethanol with a few drops of acetic acid until the background was clear. Subsequently, the sections were dehydrated in 100% ethanol, cleared in xylene, and mounted in PDX Permount (Sigma-Aldrich). Finally, the sections were photographed at both low (4x) and high (20x) magnification under bright-field illumination (BX43; Olympus).

## 2.7. Quantitative real-time PCR

Mice were deeply anesthetized and transcardially perfused with 20 ml PBS. The hippocampus was then dissected from the brain and analyzed by qPCR. Total RNA was extracted using TRIzol reagent (Invitrogen) and reverse transcribed using a PrimerScript™ RT Master Mix (Takara clontech, Mountain view, CA, USA) following the manufacturer's instructions. Quantitative real-time PCR was performed using 2x Universal SYBR Green Fast qPCR Mix (ABclonal, Woburn, MA, USA) and performed by StepOnePlus real-time PCR system (Applied Biosystems, Foster city, CA, USA). The primer sequence information is enlisted in Table 1. After normalization using the housekeeping gene *Rn18s*, raw data were analyzed using the comparative cycle threshold method. Data were reported as fold changes in mRNA levels in treated samples relative to control.

**Table 1. Primer sequence for qPCR**

Target	Sequence
Mouse <i>Ccl2</i>	Forward: 5' - CAC TCA CCT GCT GCT ACT CA- 3' Reverse: 5' - GCT TGG TGA CAA AAA CTA CAG C- 3'
Mouse <i>Cd68</i>	Forward: 5' -ACT GGT GTA GCC TAG CTG GT- 3' Reverse: 5' - CCT TGG GCT ATA AGC GGT CC- 3'
Mouse <i>Clec7a</i>	Forward: 5' -ATG GTT CTG GGA GGA TGG AT- 3' Reverse: 5' -CCT GGG GAG CTG TAT TTC TG- 3'
Mouse <i>C1qa</i>	Forward: 5' -CAA AGG AGA GAG AGG GGA GC- 3' Reverse: 5' -GGT CCC TGA TAT TGC CTG GA- 3'
Mouse <i>Gfap</i>	Forward: 5' -AGA AAG GTT GAA TCG CTG GA- 3' Reverse: 5' -CGG CGA TAG TCG TTA GCT TC- 3'
Mouse <i>Ifn-β</i>	Forward: 5' -TTC CTG CTG TGC TTC TTC AC- 3' Reverse: 5' -CTT TCC ATT CAG CTG CTC CA- 3'
Mouse <i>Rsad2</i>	Forward: 5' -CTT CAA CGT GGA CGA AGA CA- 3' Reverse: 5' -ATT CAG GCA CCA AAC AGG AC -3'
Mouse <i>Ifit1</i>	Forward: 5' -AGG CTG GAG TCT GCT GAG AT -3' Reverse: 5' -TCT GGA TTT AAC CGG ACA GC- 3'
Mouse <i>Stat1</i>	Forward: 5' -TGA TTG ACC TGG AGA CCA CC- 3' Reverse: 5' -TCA ACA CCT CTG AGA GCT GG- 3'
Mouse <i>Ch25h</i>	Forward: 5' -GCG ACC CAA TAC ATG AGC TT- 3' Reverse: 5' -CAA AGG GCA CAA GTC TGT GA- 3'
Mouse <i>Rn18s</i>	Forward: 5' -CGC GGT TCT ATT TTG TTG GT- 3' Reverse: 5' -AGT CGG CAT CGT TTA TGG TC- 3'

## 2.8. Flow cytometry

The hippocampus was dissected from the brain, homogenized in RPMI medium, and incubated with Collagenase IV (Sigma-Aldrich) and DNase I (New England Biolabs, Ipswich, MA, USA) in a shaking incubator at 37°C for 30 minutes. Enzyme activity was stopped with ice-cold PBS, and homogenates were filtered using Falcon® 5 ml round bottom polystyrene test tubes with cell strainer snap caps (Corning, Glendale, AZ, USA). Homogenates were centrifuged and resuspended with 30% Percoll (Sigma-Aldrich). 1X HBSS was then carefully added above the Percoll layer. Following centrifugation at 700 g for 30 minutes at room temperature, cell debris and myelin were carefully removed. The cells were washed thoroughly and stained with anti-CD45 antibody (1:500), anti-CD11b (1:500) antibody, and DAPI. Flow cytometric analyses were then performed using a flow cytometer (Verse I cell analyzer, BD bioscience) and analyzed using FlowJo software (TreeStar).

## 2.9. Western blot and ELISA

Total proteins were extracted from hippocampus in RIPA buffer containing 50 mM Tris-Cl (pH 8), 150 mM NaCl, 0.1% SDS, 1 mM EDTA, 1% Triton X-100, 0.05% sodium deoxycholate, and protease inhibitors. The protein concentrations were measured using Bradford assay. Protein samples were separated by 8-10% SDS-polyacrylamide gel electrophoresis and then transferred to PVDF membranes. Next, the membranes were briefly washed with PBST and blocked with 3% skim milk at room temperature for one hour, followed by incubation with anti-STAT1 (1:1000), anti-IRF9 (1:1000), anti-Viperin (1:500), and anti- $\beta$ -actin (1:1000) antibodies. The membranes were then washed with PBST and incubated with horseradish peroxidase-conjugated secondary antibodies for 1-2 hours at room temperature. After washing, the corresponding secondary antibodies were visualized using Pierce™ ECL Western Blotting Substrate (Thermo Fisher Scientific). Visualization of the blots was conducted using the ImageQuant™ 800, and images were cropped for presentation.

The remaining protein samples were used to measure the IFN- $\beta$  cytokine levels using the Mouse IFN- $\beta$  ELISA kit (Biolegend).

## 2.10. Statistical analysis

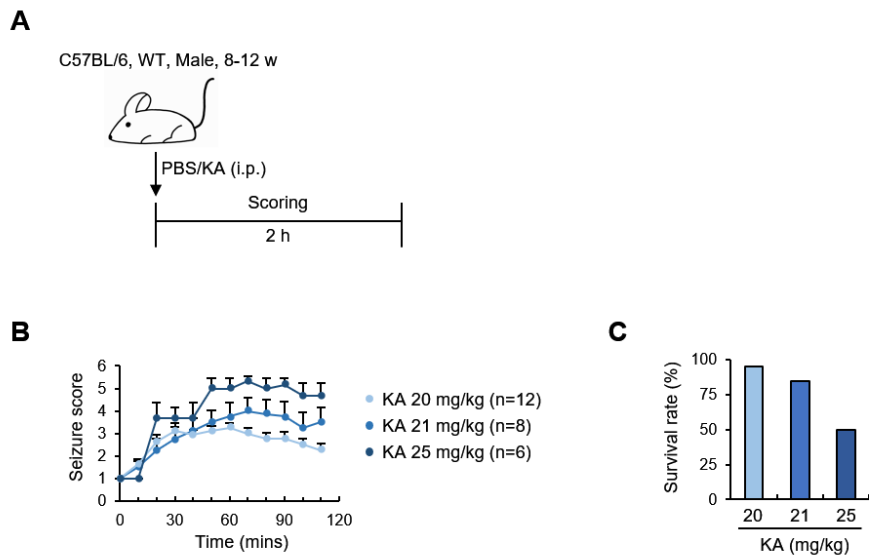
All data are presented as the mean  $\pm$  standard error of the mean (SEM) of individual samples. Data were statistically evaluated using several tests to ensure robust analysis. For comparisons between two groups, the Student's t-test was employed. The Mann-Whitney *U* test was used for seizure score comparisons between WT and *Ifnar1* knockout mice. For survival analysis, the Gehan-Breslow-Wilcoxon test was used to compare survival curves. For experiments involving multiple factors, two-way analysis of variance (ANOVA) was applied, followed by post hoc Tukey's test to explore interactions between the factors. P-values  $< 0.05$  were considered statistically significant (\* $p < 0.05$ , \*\* $p < 0.01$ , \*\*\* $p < 0.001$ , \*\*\*\* $p < 0.0001$ ). All statistical analyses were performed using Prism 9.0 (GraphPad Software).

## 3. Results

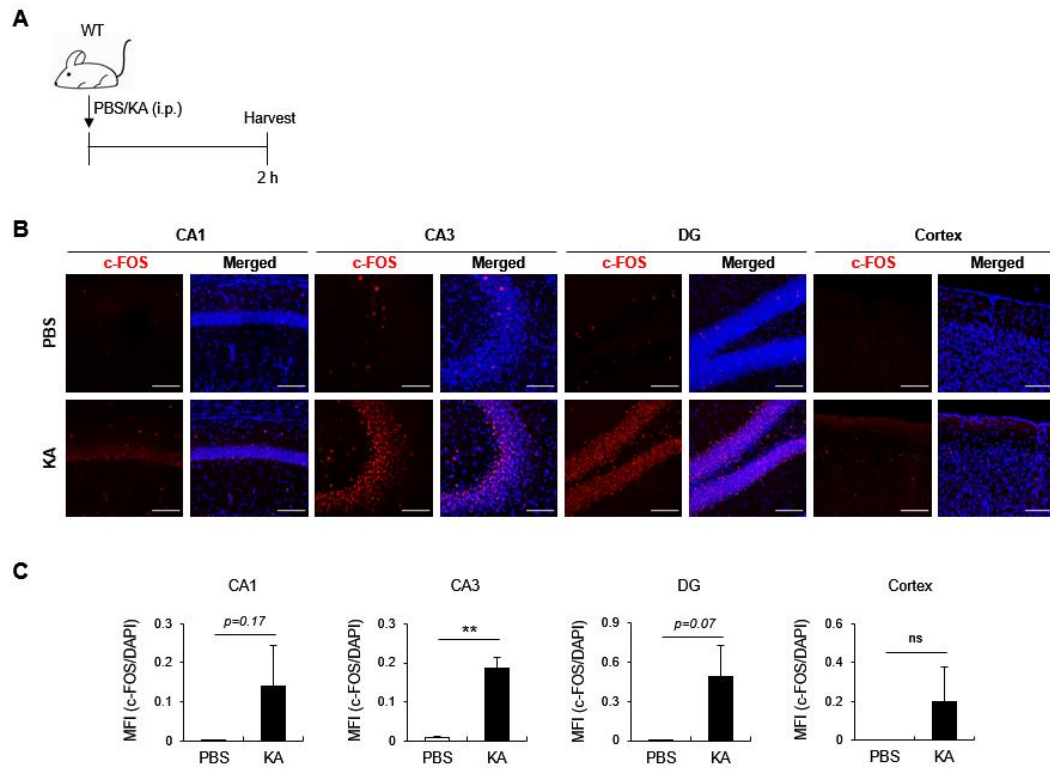
### 3.1. Kainic acid injection induces neural hyperactivity and the development of seizures

To induce acute seizures in mice, we used kainic acid (KA), a potent neuroexcitatory amino acid that can activate kainate receptors, which are ionotropic receptors on neurons. Since kainate receptors are specifically abundant in the hippocampus, KA injection can induce hippocampus-targeting focal seizures, leading to temporal lobe epilepsy<sup>48</sup>. We have demonstrated that the intraperitoneal injection of KA successfully induces acute seizures in C57BL/6 mice in a dose-dependent manner (Fig. 1). Considering the survival rates and the severity of seizures, a dosage of 21 mg/kg was selected as an appropriate concentration.

To further examine neuronal activation following KA injection, we assessed the expression level of c-FOS, an activated neuronal marker, in the brain. Indeed, our results reveal an increased expression pattern of c-FOS in the hippocampus and the cortex 2 hours after KA injection (Fig. 2). These results suggest a correlation between neuronal activity and behavioral seizures.



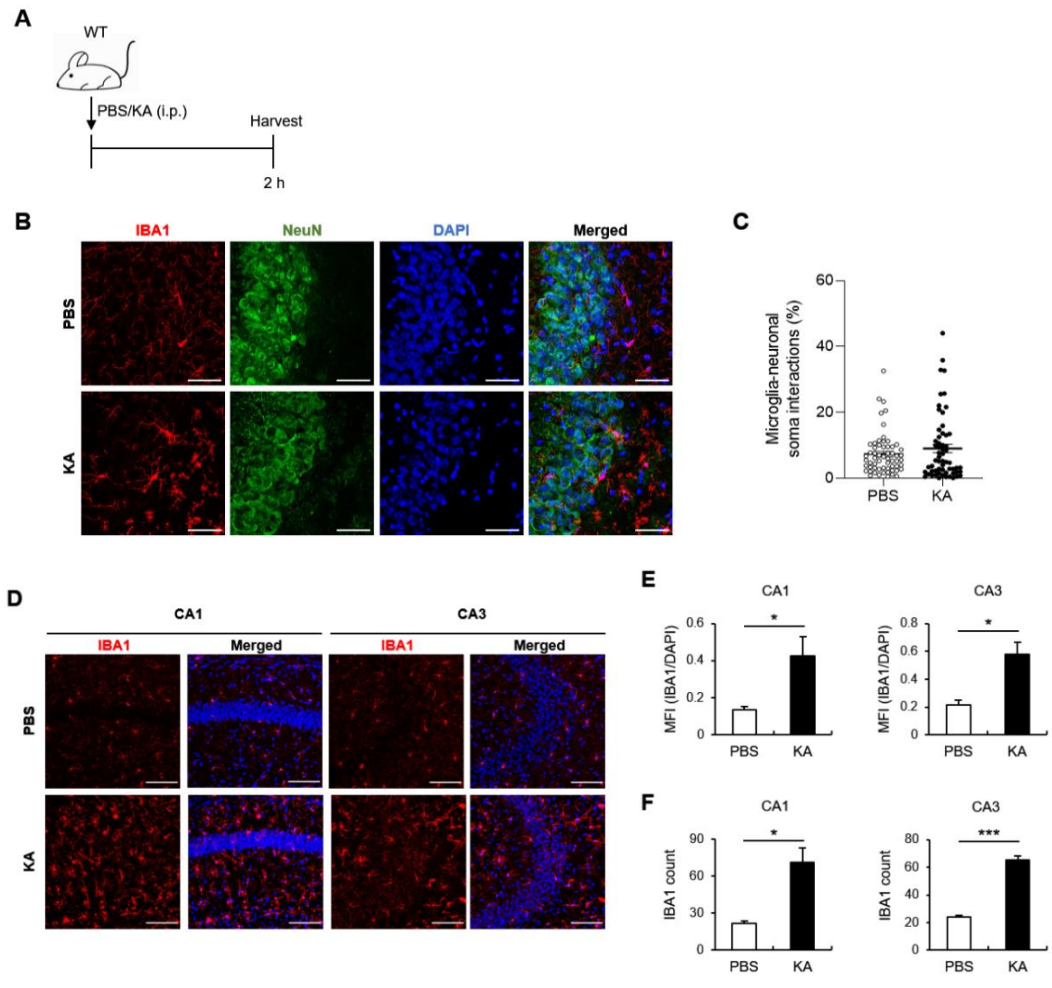
**Figure 1. Kainic acid-induced acute seizure development in mice.** (A) Eight to twelve-week-old wild-type male mice were administered intraperitoneal injection of kainic acid (20-22 mg/kg), and seizure scores were measured for 2 hours with 10-minute intervals. (B, C) Seizure scores over time and survival rates with various doses. KA; Kainic acid



**Figure 2. Increased expression pattern of c-FOS in the hippocampus and cortex following kainic acid-induced seizures.** (A) Brain sections were collected 2 hours after seizure induction for confocal imaging. The sections were stained with anti-c-FOS antibody, and the hippocampal subregions CA1, CA3, and DG, as well as the cortex, were imaged at a magnification of 20x using z-stack imaging with an interval of 1  $\mu$ m. (B) Confocal images of c-FOS and DAPI in the hippocampus and cortex. Scale bar, 100  $\mu$ m. (C) Quantification of mean fluorescence intensity (MFI) of c-FOS<sup>+</sup> signals normalized to DAPI.

### **3.2. Microglia are activated in the acute phase of seizures**

Given previous reports indicating phenotypic alterations in microglia in response to epileptic stimuli<sup>19,21</sup>, we conducted immunohistochemistry of microglia 2 hours after KA injection (Fig. 3A). Initially, we analyzed the overlap of NeuN<sup>+</sup>, a neuronal marker, with IBA1<sup>+</sup>, a microglial marker, to investigate whether hyperexcitation of neurons induces microglial process extension towards neurons. However, no significant difference was observed in microglia-neuronal soma interactions in the CA3 region between the KA-injected and PBS-injected groups (Fig. 3B, C). On the contrary, KA administration induced a substantial increase in the mean fluorescence intensity (MFI) and the number of IBA1<sup>+</sup> cells in the hippocampal region compared to control mice, suggesting the migration of microglia towards hyperexcited neurons (Fig. 3D-F). Subsequent analysis of microglial morphology revealed enlarged cell bodies and the presence of phagocytic cups within microglia in seizure-induced mice (Fig. 3G, H). In contrast, no changes were detected in microglial processes and Sholl analysis (Fig. 3I-L).



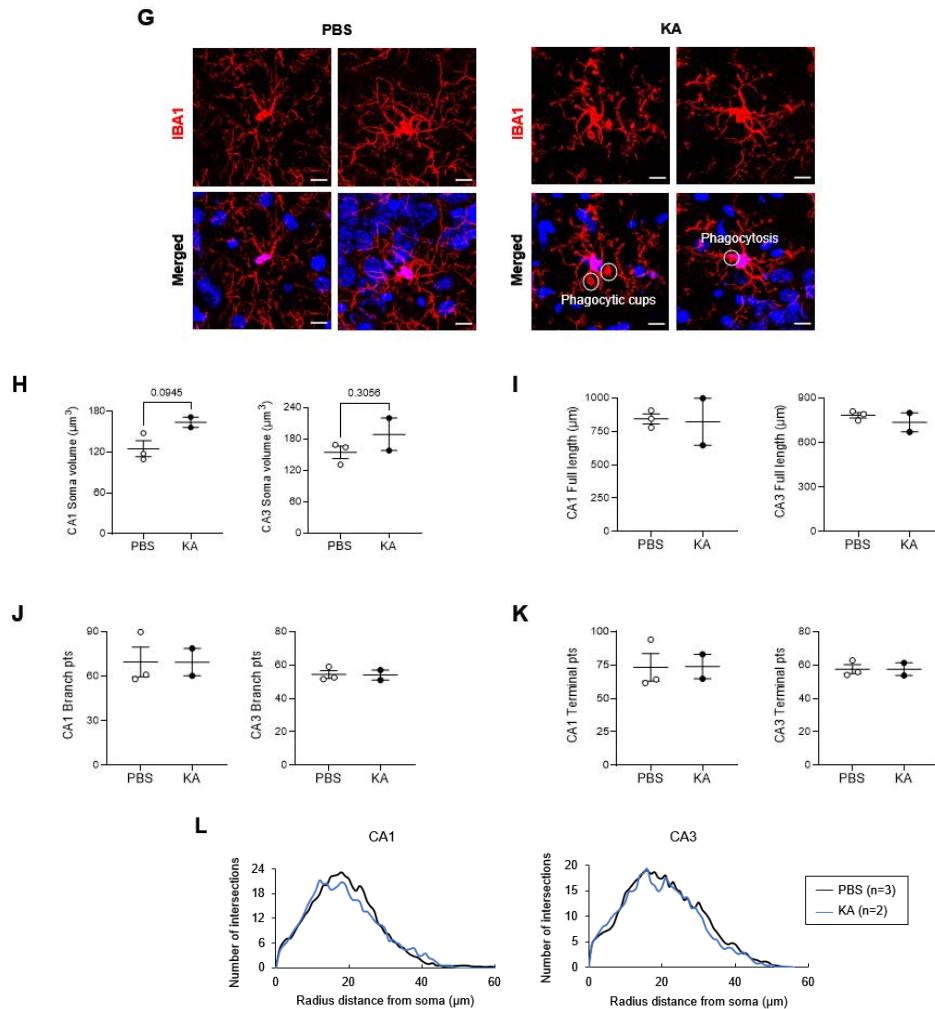


**Figure 3. Microglia activation in the acute phase of seizures.** (A) Mice were sacrificed 2 hours after seizure induction, and brain sections were used for confocal imaging. Sections were stained with anti-IBA1 and anti-NeuN antibodies. Hippocampal subregions CA1 and CA3 were imaged at magnifications of 20x or 40x using z-stack imaging with an interval of  $0.75 \mu\text{m}$ . (B) Confocal images of IBA1, NeuN, and DAPI in the CA3 region. Scale bar,  $50 \mu\text{m}$ . (C) Quantification of the percentage of microglia-neuronal soma interactions in CA3. 20-30 neurons were chosen per mouse, and the IBA1<sup>+</sup> area within each neuron was calculated. (D) Confocal images of IBA1 and DAPI in the CA1

and CA3 regions of PBS- or KA-injected mice. Scale bar, 100  $\mu\text{m}$ . (E, F) Quantification of mean fluorescence intensity (MFI) of IBA1<sup>+</sup> signals normalized to DAPI and the IBA1<sup>+</sup> cell count in the image. (G) Representative images of microglia in PBS- or KA-injected mice. Scale bar, 10  $\mu\text{m}$ . (H) Quantification of microglial soma volume in the CA1 and CA3 regions. (I-L) Quantification of full length, the number of branch points and terminal points, and Sholl analysis of microglial processes in the CA1 and CA3 regions.

### 3.3. Kainic acid injection induces neuronal death and gliosis in the late phase of seizures

To examine the long-term effects of KA-induced seizures, we analyzed representative late phase seizure phenotypes, neuronal death and gliosis, at various time points (Fig. 4A). We utilized the TUNEL assay and Nissl staining, representing apoptotic cells and living neurons, respectively. Both analyses showed that cell death, particularly neuronal death, occurred specifically at 3 and 7 days after seizures, although this was not statistically significant (Fig. 4B-D).

Next, we performed immunohistochemistry of microglia and astrocytes to assess the reactivity of glial cells in the late phase of seizures (Fig. 5). Indeed, the number of IBA1<sup>+</sup> microglia in the CA1 and CA3 regions showed a slight increase in KA-injected mice, with an enlargement of the soma area observed specifically 3 and 7 days after KA injection, although not statistically significant (Fig. 5C). Additionally, the number of astrocytes, represented by GFAP, gradually increased after KA injection compared to control mice in CA1 and CA3, suggesting an increasing tendency (Fig. 5D).

To further confirm gliosis, we analyzed the mRNA levels in the hippocampus one day after KA administration. Genes involved in chemoattraction (*Ccl2*), microglia activation (*Cd68*, *Clec7a*), phagocytosis (*C1qa*), and astrocyte activation (*Gfap*) were assessed. The gene expressions showed an upregulated pattern in the hippocampus of seizure-induced mice (Fig. 6).

Since the mRNA level of the chemoattractant gene was increased and a previous study indicated that infiltrating monocytes accelerate brain inflammation and neuronal damage after status epilepticus<sup>49</sup>, we analyzed changes in cell numbers of microglia and infiltrating immune cells via flow cytometric analysis (Fig. 7). As a result, in contrast to control mice, seizure-induced mice showed an increased pattern in the number of microglia and infiltrating immune cells in the hippocampus 7 days post-KA injection. Furthermore, the expression of CD45 and CD11b was increased in microglia, implying microglia activation. Therefore, we conclude that neuronal death, glia activation, and immune cell infiltration occur in the late phase of seizures.

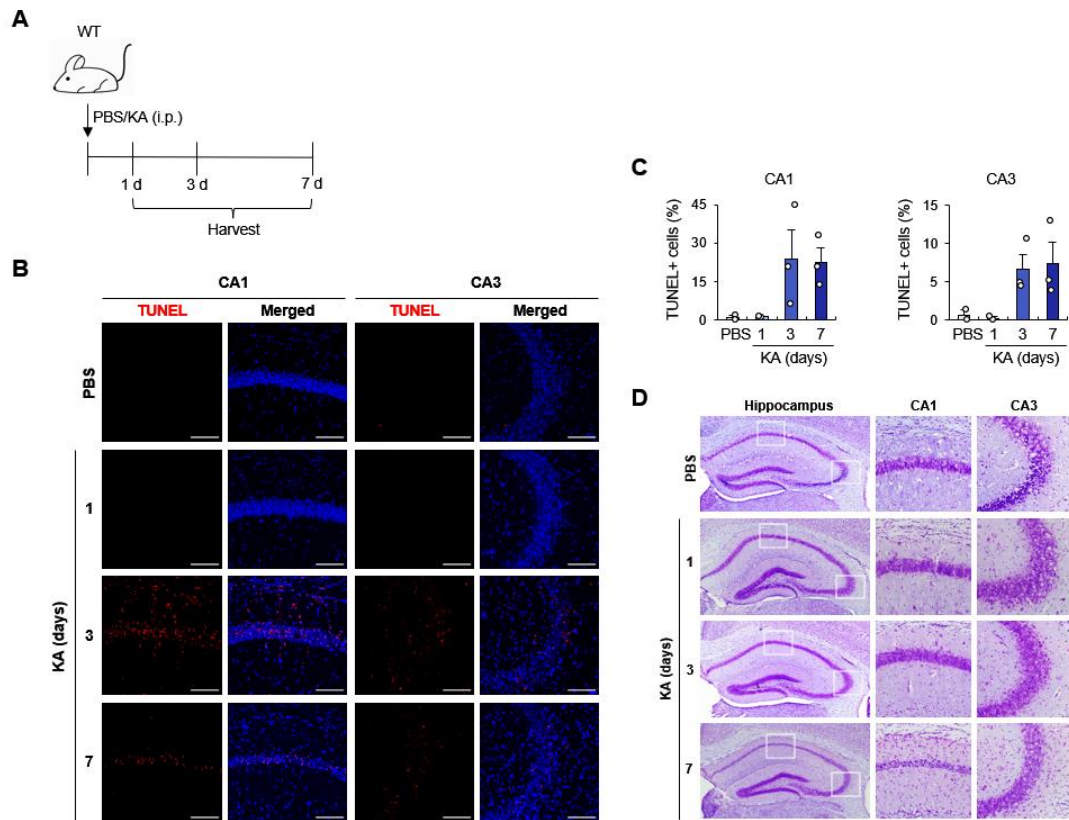


**Figure 4. Neuronal death in the late phase of seizures.** (A) Mice were sacrificed 1, 3, and 7 days after seizure induction, and brain sections were used for TUNEL assay and Nissl staining. For the TUNEL assay, CA1 and CA3 regions were imaged at a magnification of 20x using z-stack imaging with an interval of 1  $\mu$ m. For Nissl staining, the hippocampus was imaged at a magnification of 4x, and the CA1 and CA3 subregions were imaged at a magnification of 20x. (B) Confocal images of TUNEL and DAPI staining in the hippocampus. Scale bar, 100  $\mu$ m. (C) Quantification of TUNEL<sup>+</sup> cells in CA1 and CA3 by calculating the ratio of TUNEL<sup>+</sup> cells to the number of nuclei (DAPI). (D) Representative images of Nissl staining in the hippocampus, CA1, and CA3.

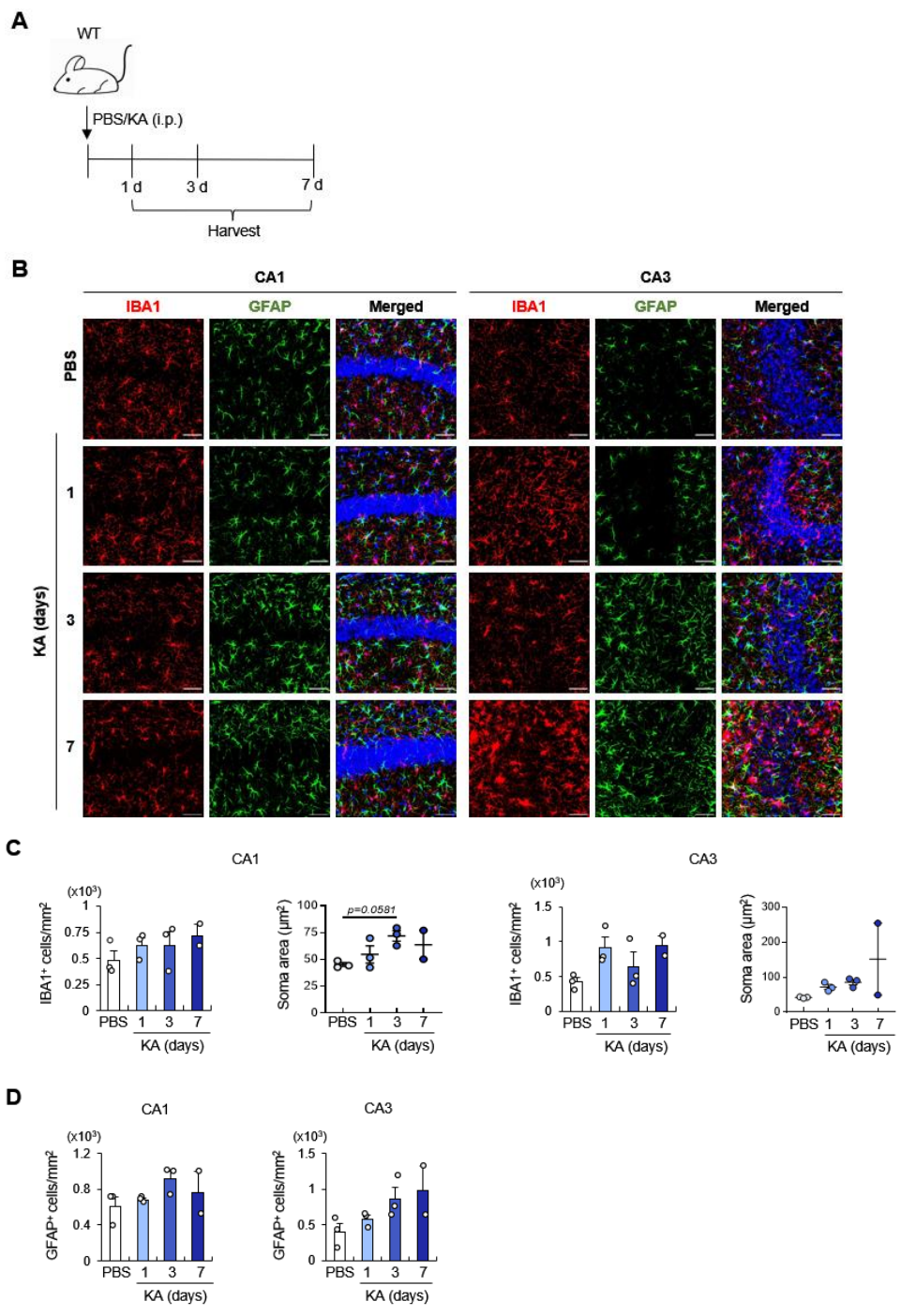


**Figure 5. Gliosis in the late phase of seizures.** (A) Brain sections were acquired at various time points, and each sample was imaged at a magnification of 20x using z-stack imaging with an interval of 1  $\mu\text{m}$ . The sections were stained with anti-IBA1 and anti-GFAP antibodies. (B) Confocal images of IBA1, GFAP, and DAPI in CA1 and CA3. Scale bar, 100  $\mu\text{m}$ . (C) Quantification of the number of IBA1<sup>+</sup> cells and the soma area of microglia in CA1 and CA3. (D) Quantification of the number of GFAP<sup>+</sup> cells in CA1 and CA3.

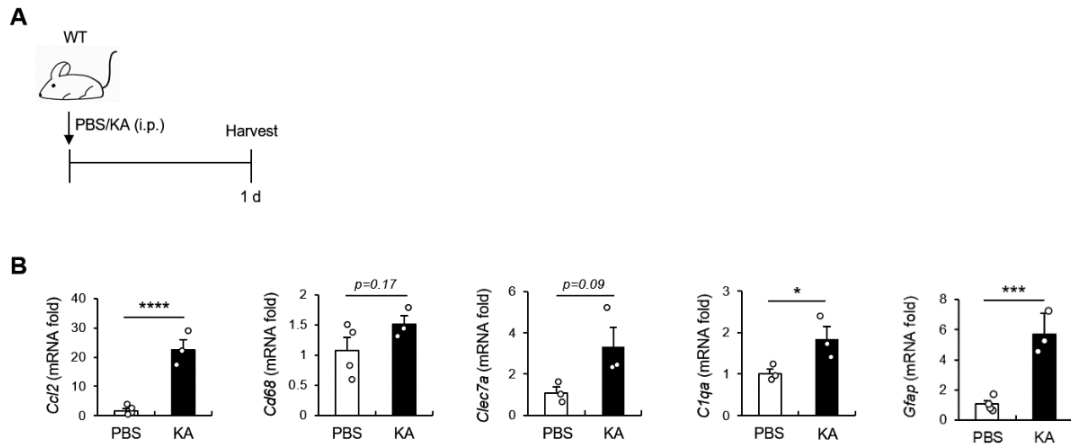


**Figure 6. Glia activation in the late phase of seizures.** (A) Mice were sacrificed one day after seizure induction, and the hippocampus was dissected for quantitative real-time PCR. (B) mRNA expression levels of target genes in the hippocampus.

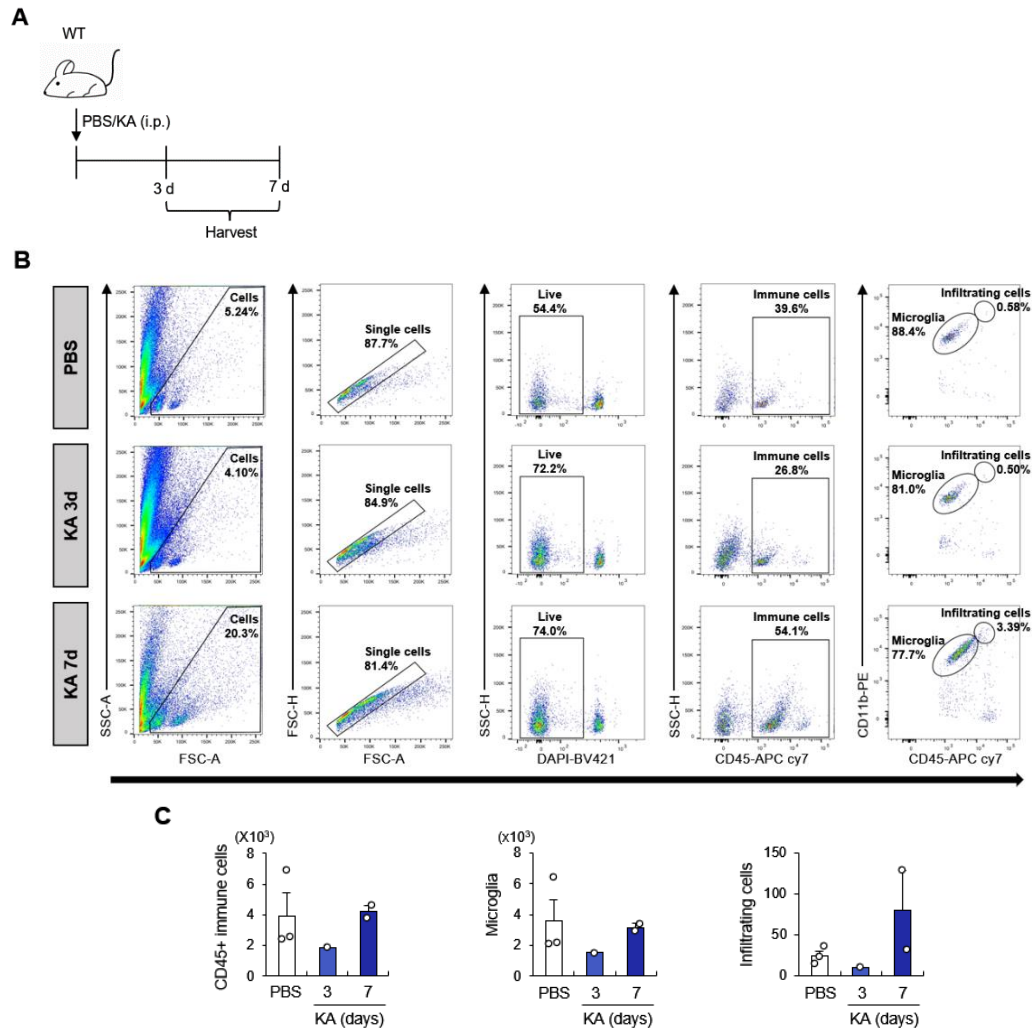


**Figure 7. Microglia proliferation and immune cell infiltration in the late phase of seizures.** (A) Mice were sacrificed 3 and 7 days after seizure induction, and the hippocampus was dissected for flow cytometry analysis. (B) Gating strategies for flow cytometric analysis of immune cells (CD45<sup>+</sup>), microglia (CD45<sup>+</sup> CD11b<sup>int</sup>), and infiltrating myeloid cells (CD45<sup>+</sup> CD11b<sup>hi</sup>) in the hippocampus. (C) Quantification of these cell numbers in the hippocampus.

### **3.4. Type I interferon signaling is activated during the late phase of seizures in the hippocampus**

We have so far shown various phenotypes of seizures. We hypothesized that type I IFN signaling might be related to these phenotypes during the initiation and progression of seizures. To examine this, we analyzed the hippocampus during the acute and late phases of seizures. During the acute phase of seizures, the mRNA level of IFN- $\beta$  was slightly upregulated without significance, but there were no alterations in the mRNA levels of interferon-stimulated genes (ISGs). Similarly, the cytokine level of IFN- $\beta$  remained unchanged, and there was no ISG production at the protein level during seizures (Fig. 8). However, one day after seizures, there were increasing patterns in the mRNA levels of IFN- $\beta$  and ISGs. Furthermore, STAT1 and viperin, which are ISGs, were upregulated in western blot analysis (Fig. 9). These results imply that type I IFN signaling might play a role in the seizure progression.

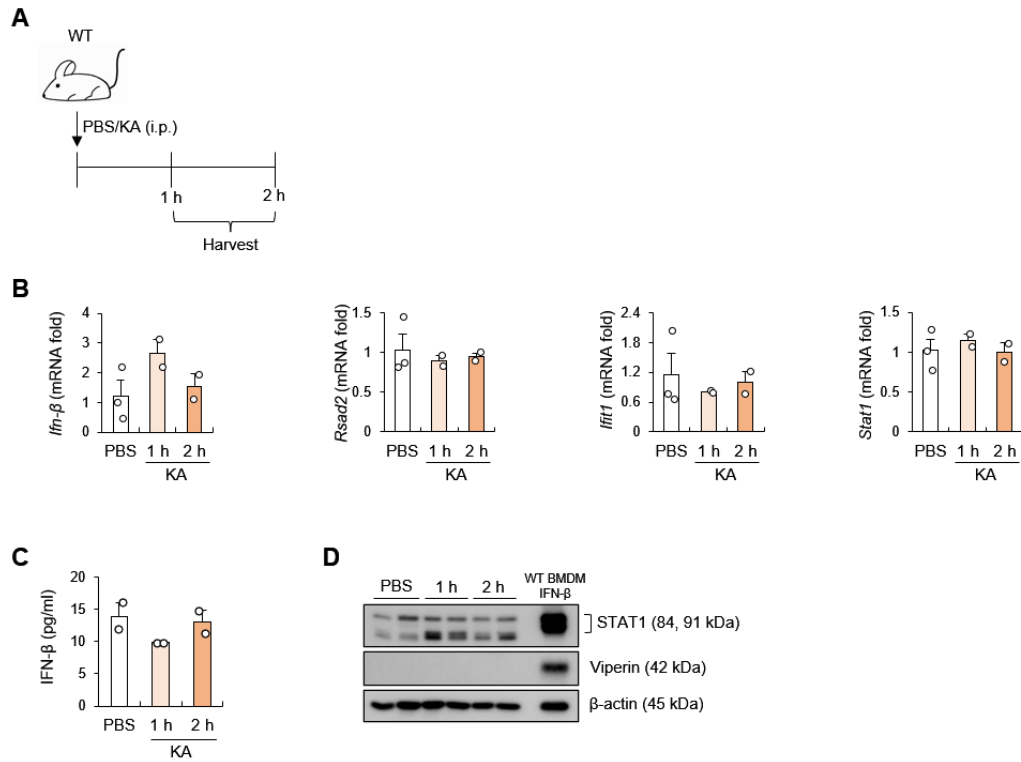


**Figure 8. Lack of type I interferon signaling in the hippocampus during seizures.** (A) Mice were sacrificed 1 and 2 hours after seizure induction, and the hippocampus was used for qPCR, ELISA, and western blot analysis. (B) mRNA levels of IFN- $\beta$  and ISGs. (C) Levels of IFN- $\beta$  protein in the hippocampus. (D) Western blot analysis of ISGs in the hippocampus.

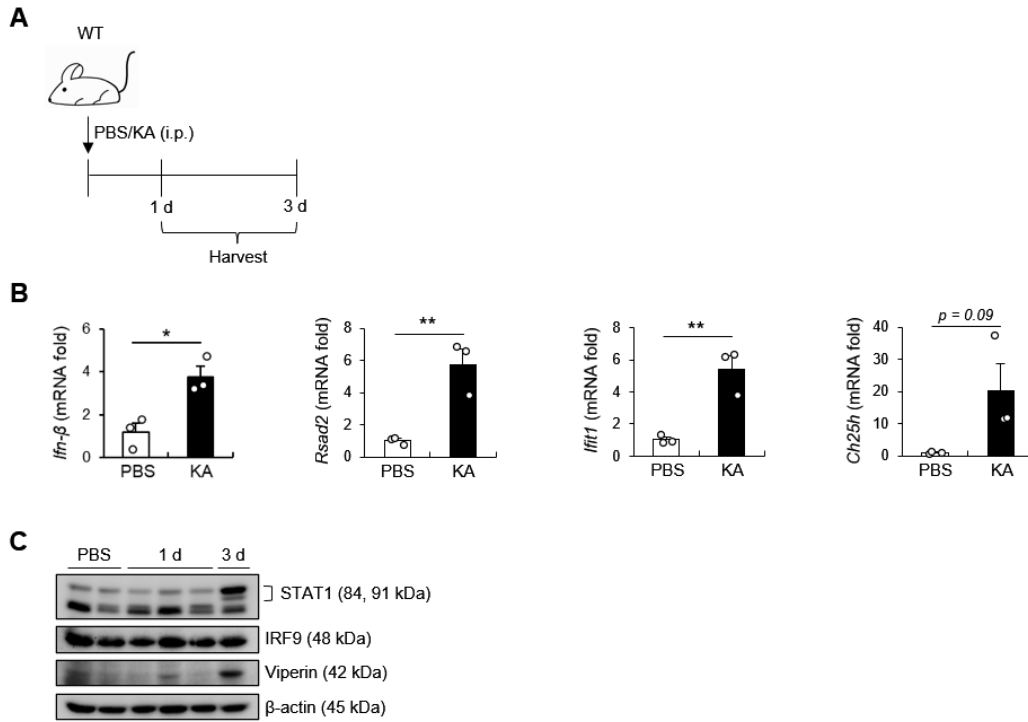


**Figure 9. Type I interferon signaling activation in the hippocampus after seizures.** (A) Hippocampal tissue was collected from mice 1 and 3 days after seizure induction for qPCR and western blot analysis. (B) mRNA expression levels of IFN- $\beta$  and ISGs 1 day after seizure induction. (C) Western blot analysis of ISGs 1 and 3 days after seizure induction.

### **3.5. Kainic acid-induced seizures are attenuated in *Ifnar1* knockout mice**

We have confirmed that type I IFN signaling is activated in the hippocampus of seizure-induced mice. To further examine the specific roles of type I IFN signaling in seizures, we induced seizures in both wild-type mice and *Ifnar1* knockout mice, which lack the type I IFN receptor, and compared the severity of seizures (Fig. 10A). Interestingly, *Ifnar1* knockout mice exhibited decreased seizure severity compared to wild-type mice (Fig. 10B). Similarly, the percentage of status epilepticus, defined as seizure scores remaining over 4 for at least 30 minutes, was lower in *Ifnar1* knockout mice than in wild-type mice (Fig. 10C). While the mortality rate and incidence rate of seizures were comparable between wild-type and *Ifnar1* knockout mice, *Ifnar1* knockout mice showed a tendency for earlier mortality during the onset of seizures within 2 hours (Fig. 10D-F). To monitor the duration of seizure aftereffects, we measured body weight daily for a week and found that weight loss was more severe in wild-type mice (Fig. 10G). Therefore, we conclude that seizure severity is alleviated in *Ifnar1* knockout mice, but they show higher susceptibility to mortality during the onset of seizures.

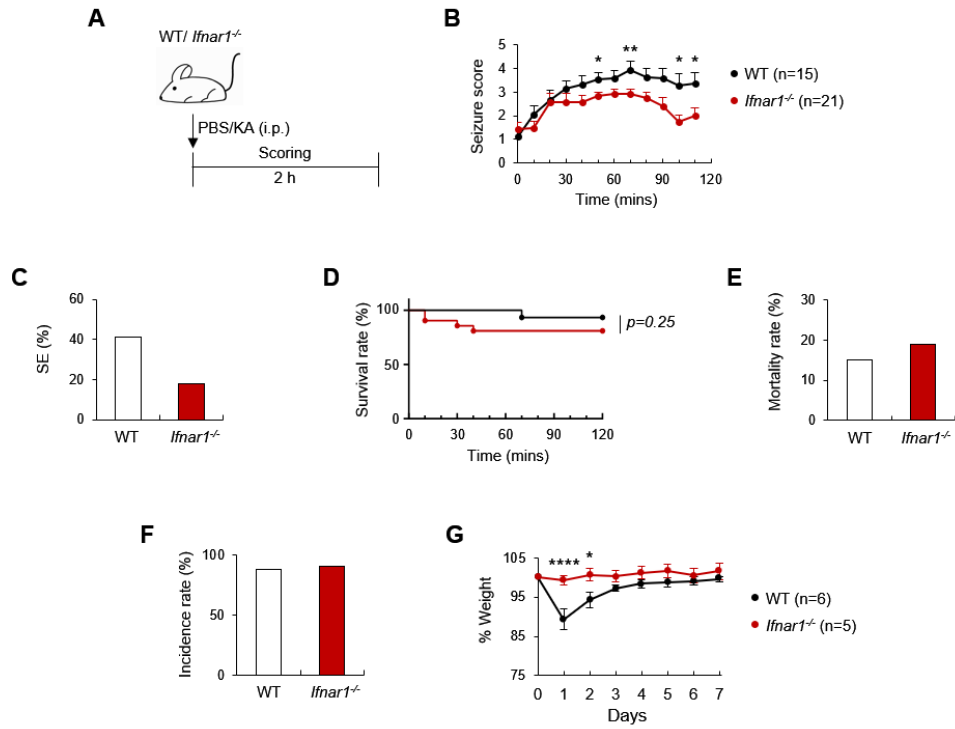


**Figure 10. Decreased seizure severity in *Ifnar1* knockout mice.** (A) WT and *Ifnar1*<sup>-/-</sup> mice were administered kainic acid, and seizure scores were measured for 2 hours. (B) Seizure scores in WT and *Ifnar1*<sup>-/-</sup> mice. (C) Percentage of status epilepticus. (D) Survival rate for 2 hours after KA injection in WT and *Ifnar1*<sup>-/-</sup> mice. (E, F) Incidence rate and mortality rate in WT and *Ifnar1*<sup>-/-</sup> mice. (G) Weight loss after KA injection in WT and *Ifnar1*<sup>-/-</sup> mice.

### **3.6. The absence of type I interferon signaling reduces neuronal activity and microgliosis in the acute phase of seizures**

We have previously confirmed the correlation between neuronal activity and behavioral seizures. To investigate whether reduced neuronal activation is observed in *Ifnar1* knockout mice, we compared c-FOS expression in the brains of WT and *Ifnar1* knockout mice after KA administration. While the PBS-injected groups rarely showed c-FOS expression in both WT and *Ifnar1* knockout mice, *Ifnar1* knockout mice exhibited decreased pattern of c-FOS expression in the hippocampal subregions CA1, CA3, and DG, as well as in the cortex compared to WT mice within the KA-injected groups (Fig. 11).

To explore whether reduced neuronal activation is associated with microglial activity, we compared the MFI of IBA1 and the number of microglia in the hippocampus of PBS- or KA-injected mice between WT and *Ifnar1* knockout mice. Both WT and *Ifnar1* knockout mice showed tendency of an increase in MFI and microglial cell count in the KA-injected groups. However, KA-injected *Ifnar1* knockout mice showed a lower increase compared to WT mice in the CA1 region (Fig. 12). These findings suggest that the reduced severity of seizures observed in *Ifnar1* knockout mice may be linked to decreased neuronal activity, possibly mediated by altered microglial activation.

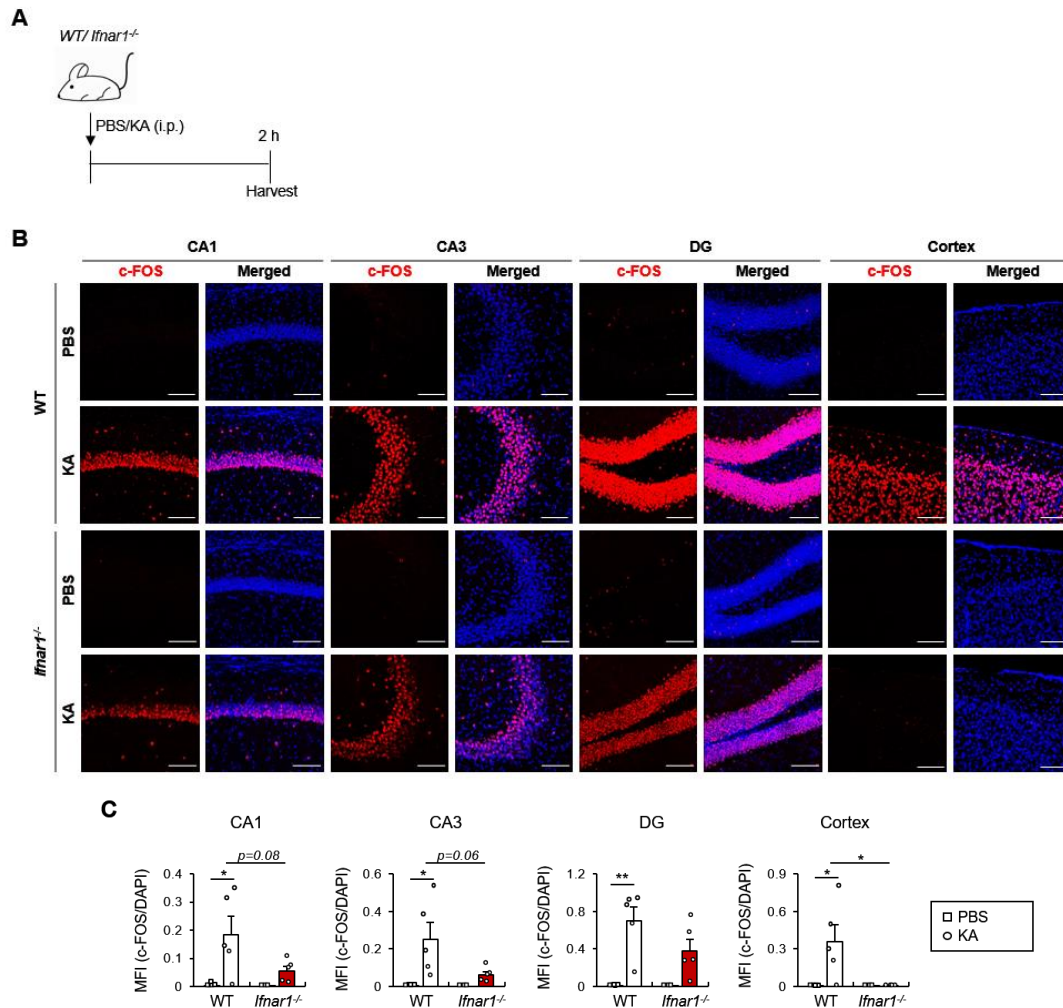


**Figure 11. Decreased c-FOS expression with loss of type I interferon signaling following kainic acid-induced seizures.** (A) WT and *Ifnar1*<sup>-/-</sup> mice were sacrificed 2 hours after seizure induction and neuronal activation was compared between them. (B) Confocal images of c-FOS and DAPI in the hippocampal subregions CA1, CA3, and DG, as well as in the cortex of WT and *Ifnar1*<sup>-/-</sup> mice. Scale bar, 100  $\mu$ m. (C) Quantification of MFI of c-FOS<sup>+</sup> signals normalized to DAPI.

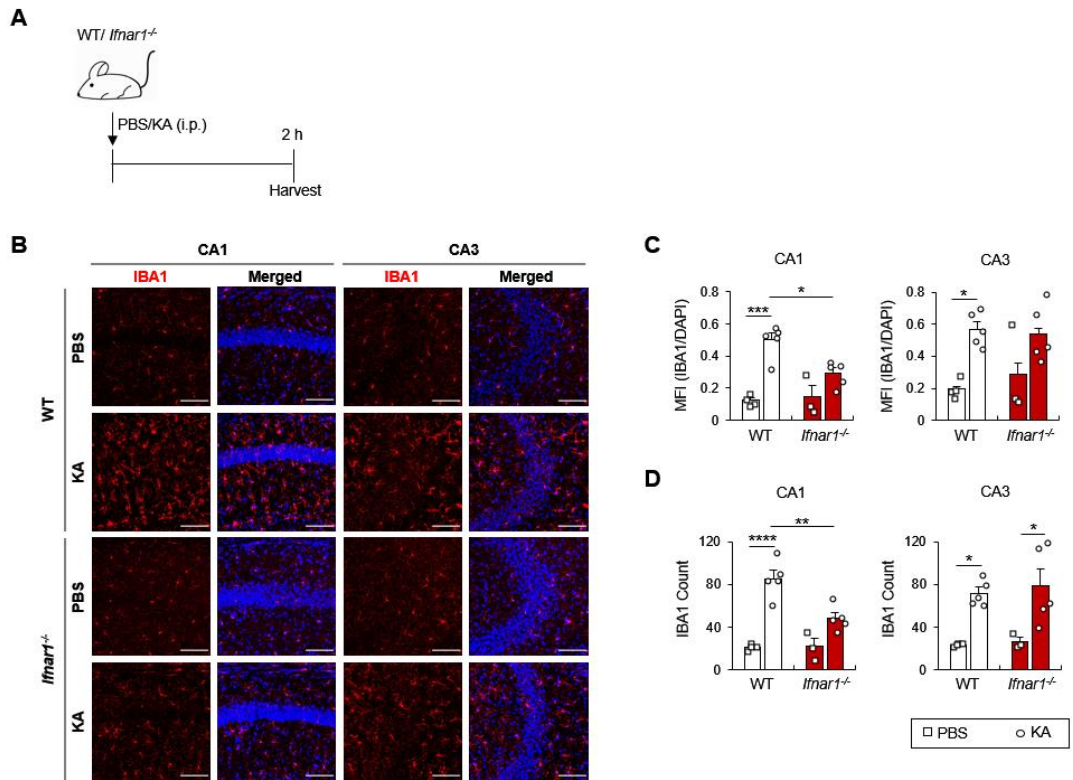


**Figure 12. Altered microglial activation due to loss of type I interferon signaling following kainic acid-induced seizures.** (A) WT and *Ifnar1*<sup>-/-</sup> mice were sacrificed 2 hours after seizure induction and microglial activation was compared between them. (B) Confocal images of IBA1 and DAPI in the hippocampal subregions CA1 and CA3 of WT and *Ifnar1*<sup>-/-</sup> mice. Scale bar, 100  $\mu$ m. (C) Quantification of MFI of IBA1<sup>+</sup> signals normalized to DAPI. (D) Quantification of the number of IBA1<sup>+</sup> cells in the images.

### **3.7. There was no significant difference in neuronal death and gliosis between WT and *Ifnar1* knockout mice during the late phase of seizures**

As observed in previous data, we found that type I IFN plays a role in the acute phase of seizures. To investigate its effects on seizure phenotypes during the late phase, we compared neuronal death and gliosis in WT and *Ifnar1* knockout mice. Interestingly, in contrast to the differences observed in the acute phase, a meaningful difference in neuronal death and gliosis was not detected 7 days after seizures. Cell death was rarely observed in either WT or *Ifnar1* knockout mice, as analyzed by TUNEL assay (Fig. 13). Additionally, the number of microglia and MFI of GFAP were not considerably different between WT and *Ifnar1* knockout mice (Fig. 14). When analyzing the morphology of microglia, we observed a tendency of increase in soma volume under seizure conditions in both WT and *Ifnar1* knockout mice, implying microglial activation. However, there was no significant difference in microgliosis between the KA-injected groups of WT and *Ifnar1* knockout mice. Sholl analysis also revealed microgliosis in KA-induced mice in both WT and *Ifnar1* knockout groups, but no difference was observed between WT and *Ifnar1* knockout mice (Fig. 15). Consequently, there was a negligible difference between WT and *Ifnar1* knockout mice during the late phase of seizures, contrary to the observation of type I IFN activation in the late phase of seizures but not in the acute phase of seizures.

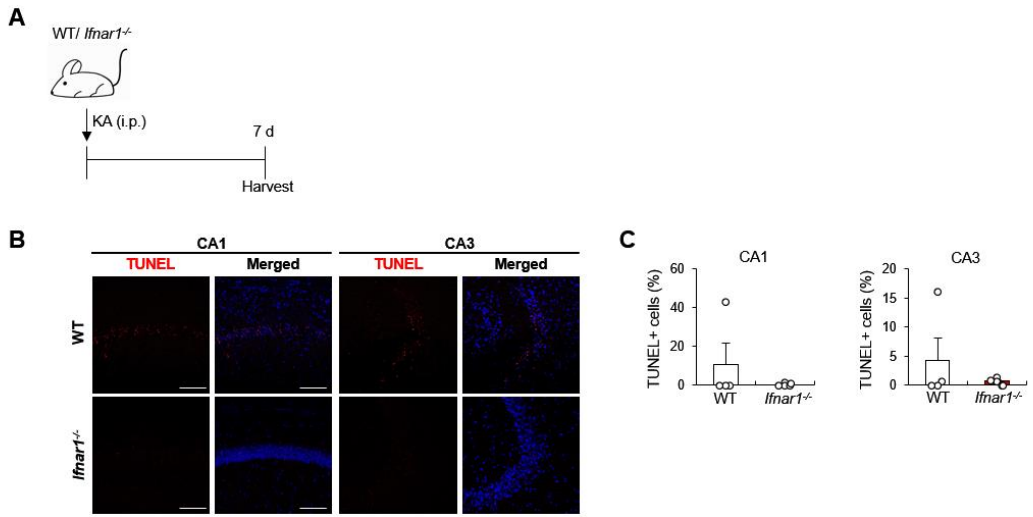


**Figure 13. Absence of neuronal death in the late phase of seizures in both WT and *Ifnar1*<sup>-/-</sup> mice.** (A) WT and *Ifnar1*<sup>-/-</sup> mice were sacrificed 7 days after seizures and neuronal death was measured through a TUNEL assay. (B) Confocal images of TUNEL and DAPI in the hippocampus. Scale bar, 100  $\mu$ m. (C) Quantification of TUNEL<sup>+</sup> cells in CA1 and CA3. The images were quantified and presented as the ratio of TUNEL<sup>+</sup> cells to the number of nuclei (DAPI).

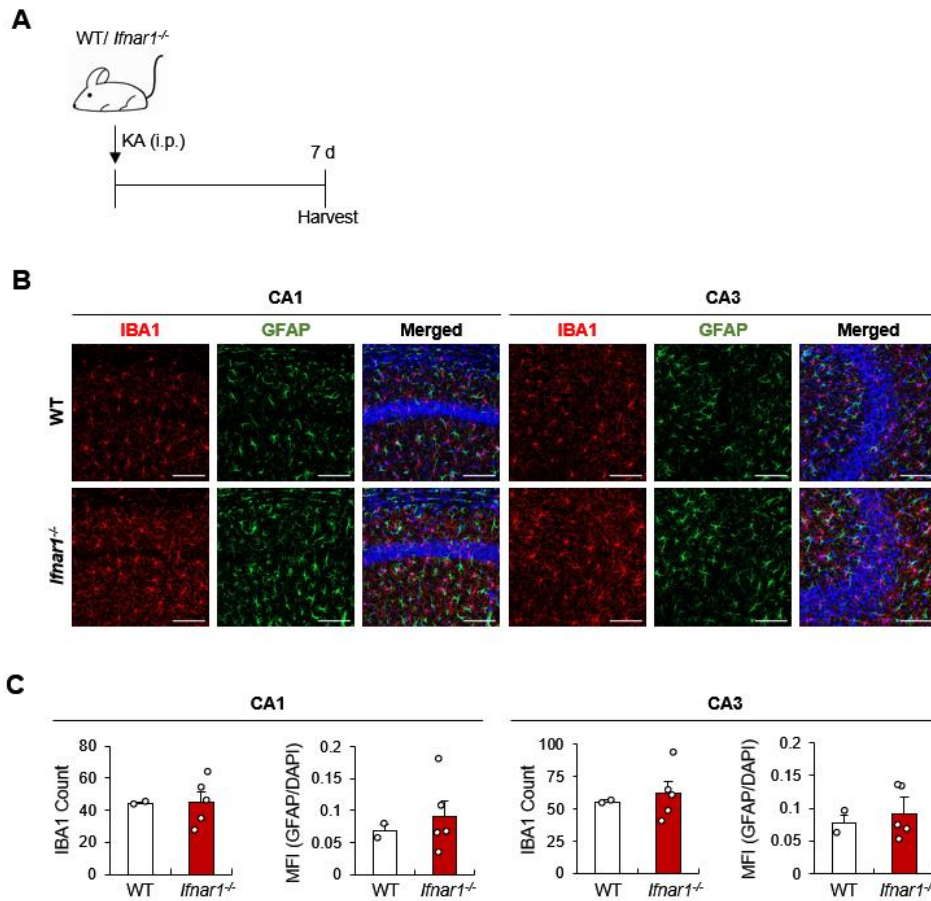


**Figure 14. Comparable gliosis levels in WT and *Ifnar1*<sup>-/-</sup> mice post-seizures.** (A) WT and *Ifnar1*<sup>-/-</sup> mice were sacrificed 7 days after seizures and gliosis was compared between them. (B) Confocal images of IBA1, GFAP, and DAPI in the hippocampus. Scale bar, 100  $\mu$ m. (C) Quantification of the IBA1<sup>+</sup> cell numbers and MFI of GFAP normalized DAPI in CA1 and CA3.

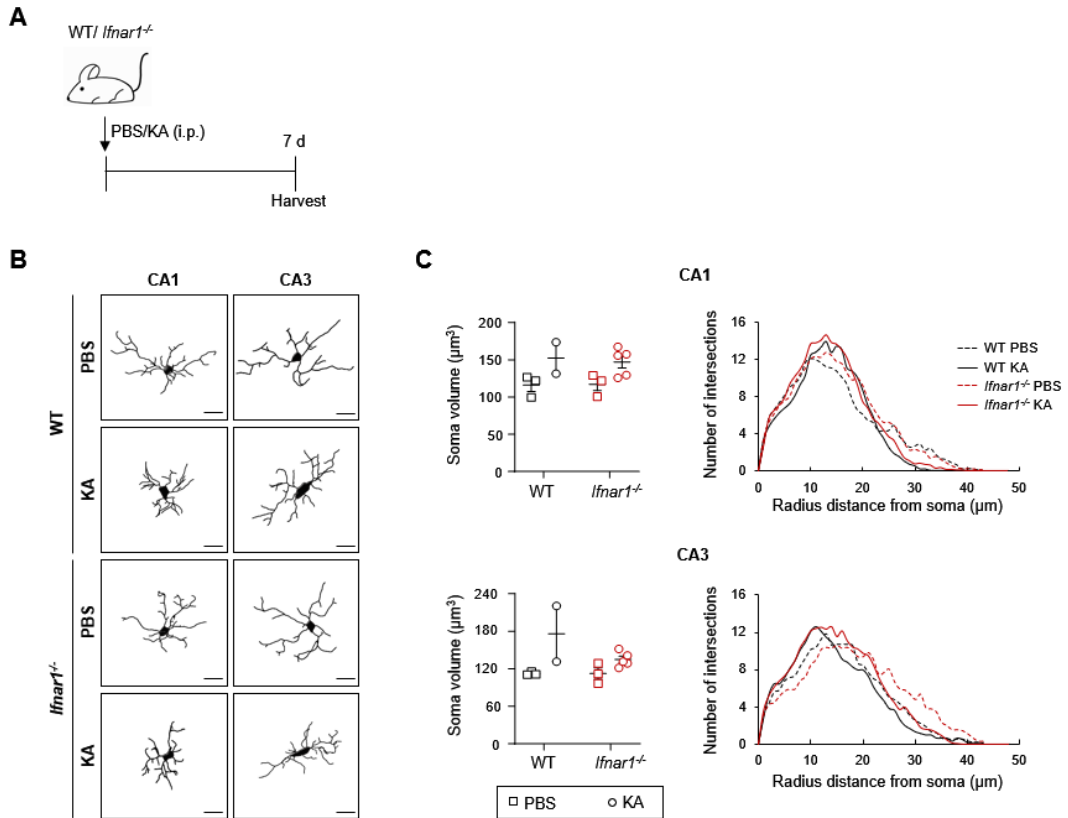


**Figure 15. No notable difference in microglia morphology between WT and *Ifnar1*<sup>-/-</sup> mice in the late phase of seizures.** (A) WT and *Ifnar1*<sup>-/-</sup> mice were sacrificed 7 days after seizures and microglia morphology was observed through IBA1 imaging. (B) Representative images of microglia morphology in CA1 and CA3. Scale bar, 10  $\mu\text{m}$ . (C) Quantification of soma volume and Sholl analysis of microglia in CA1 and CA3.

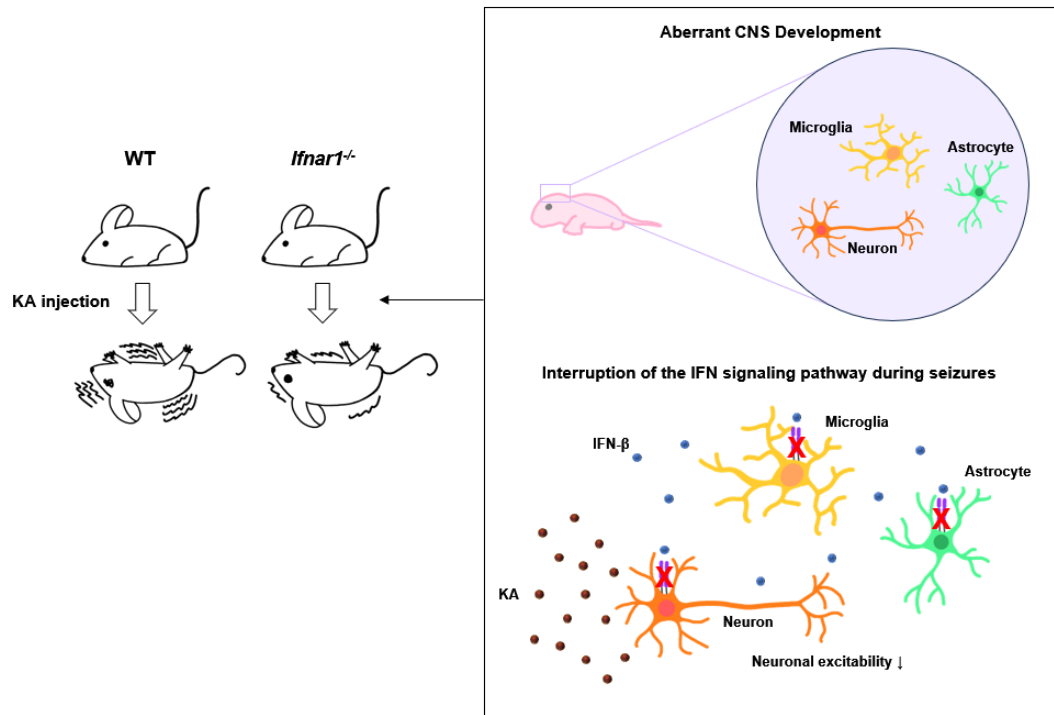


**Figure 16. Suggested explanations for reduced seizure severity in *Ifnar1<sup>-/-</sup>* mice.** The attenuation of seizure severity in *Ifnar1<sup>-/-</sup>* mice could result from either aberrant CNS development or the interruption of the IFN signaling pathway during seizures.

## 4. Discussion

Type I IFNs have been suggested as pivotal cytokines for CNS development and homeostasis. Although their impacts have been reported in various CNS diseases, there have been few studies on the relationship between seizures and type I IFN signaling. Recent studies have proposed that type I IFN signaling might play a role in the pathogenesis of seizures. However, its specific role and underlying mechanisms remain elusive. Here, we demonstrated that type I IFN signaling affects seizures, particularly in their initiation phase.

Initially, we confirmed various seizure phenotypes in both the acute and late phases. During the acute phase of seizures, neuronal activation primarily occurs in the hippocampus, and microglia migrate near the hippocampal layers and become activated. Neuronal death and gliosis were also observed during the late phase of seizures. Subsequently, we identified the activation of type I IFN signaling exclusively in the late phase, contrasting its absence during the acute phase. Furthermore, we conducted a comparative analysis of seizure phenotypes between WT and *Ifnar1* knockout mice. Interestingly, *Ifnar1* knockout mice exhibited reduced seizure severity during the acute phase of seizures. Moreover, in seizure-induced *Ifnar1* knockout mice, neuronal activation and microgliosis appeared attenuated compared to their WT counterparts during the acute phase of seizures. However, no significant differences were observed between WT and *Ifnar1* knockout mice during the late phase of seizures.

There are two possible explanations for these altered phenotypes (Fig. 16). One possibility is that since type I IFN signaling is essential during brain development, the absence of IFN signaling might lead to altered neuronal excitability and aberrant microglia properties. This alteration could affect the seizure threshold or the response of neurons in *Ifnar1* knockout mice to excess neurotransmitters. The other possibility is that although type I IFNs are present in low doses in the CNS, they might bind to IFNAR1 during seizures, potentially promoting neuronal activity and microgliosis. However, this explanation does not account for the absence of detected type I IFN signaling activation during the acute phase of seizures. It is conceivable that the activation of type I IFN signaling was not sufficiently amplified to be detected during this phase. Therefore, to validate these hypotheses, experiments involving intracerebroventricular injection of IFN- $\beta$  or ruxolitinib, a JAK inhibitor, before seizures could be conducted. By comparing the results with those of *Ifnar1* knockout

experiments, we may gain insights into the role of type I IFN signaling in seizures. Therefore, further study is warranted to ascertain which explanation is correct.

If the latter explanation is found to be reasonable, one possible mechanism of type I IFN signaling influence on the seizures involves the mTOR pathway, a non-canonical pathway of type I IFN signaling. mTOR is a serine/threonine protein kinase that forms mTOR complex 1 (mTORC1) and mTOR complex 2 (mTORC2). The mTOR pathway regulates metabolism, cell growth, survival and proliferation, and its dysregulation has been implicated in epilepsy. Tuberous sclerosis complex (TSC), caused by pathogenic variants in the *TSC1* or *TSC2* gene, results in mTOR pathway inhibition. Consequently, many patients with TSC develop drug-resistant epilepsy<sup>50</sup>. Furthermore, mTOR inhibition has been effective in suppressing seizures, and mTOR overactivation in microglia itself can induce spontaneous seizures<sup>51-53</sup>. Therefore, we speculate that type I IFN signaling activation during seizure stimulates mTORC1 and mTORC2 activation, exacerbating neuronal activation and microgliosis. To investigate this, comparisons of mTORC1 and mTORC2 activation between WT and *Ifnar1* knockout under seizure conditions could be conducted. Additionally, in vitro experiments with mixed glia could investigate mTOR activation following IFN stimulation. Furthermore, experiments could be conducted in bone marrow-derived cells (BMDMs) or peritoneal macrophages to determine if mTOR activation following IFN stimulation occurs exclusively in mixed glia.

Moreover, the specific cell types crucial for IFN signaling during seizures remain unidentified. This could be investigated using cell type-specific knockout mice or AAV virus-induced cell type-specific deletion.

Epilepsy is one of the most understudied neurological diseases, underscoring the importance of identifying novel treatment targets. In this regard, our findings, demonstrating that *Ifnar1* knockout mice exhibit attenuated seizure severity, are noteworthy and provide novel insights into disease progression.

## 5. Conclusion

Our study demonstrated that *Ifnar1* knockout mice showed reduced seizure severity compared to WT mice following kainic acid injection. During the acute phase of seizures, *Ifnar1* knockout mice exhibited reduced neuronal activity and microgliosis compared to WT mice. Despite IFN signaling being present in the late phase of seizures but absent during the acute phase, WT and *Ifnar1* knockout mice did not exhibit significant differences in phenotypes related to neuronal death and gliosis in the late phase of seizures. These findings suggest that type I IFN may influence both neuronal activation and microglial function. The altered seizure phenotypes observed in *Ifnar1* knockout mice may result from abnormalities in CNS development, the absence of IFN signaling during seizures, or both factors combined. Further studies are needed to elucidate these mechanisms and probe specific cell types relevant to these IFN signaling. Consequently, our study suggests the potential therapeutic utility of type I IFNs as a target for treating seizures and epilepsy.

## References

1. Kirschman, L. T., Borysiewicz, E., Fil, D., & Konat, G. W. (2011). Peripheral immune challenge with dsRNA enhances kainic acid-induced status epilepticus. *Metabolic brain disease*, *26*, 91-93.
2. Johnson, E. L. (2019). Seizures and epilepsy. *Medical Clinics*, *103*(2), 309-324.
3. Blazekovic, A., Gotovac Jercic, K., Meglaj, S., Duranovic, V., Prpic, I., Lozic, B., ... & Borovecki, F. (2022). Genetics of pediatric epilepsy: next-generation sequencing in clinical practice. *Genes*, *13*(8), 1466.
4. Burke Jr, K. J., & Bender, K. J. (2019). Modulation of ion channels in the axon: mechanisms and function. *Frontiers in cellular neuroscience*, *13*, 221.
5. Gandolfi, D., Bigiani, A., Porro, C. A., & Mapelli, J. (2020). Inhibitory plasticity: from molecules to computation and beyond. *International journal of molecular sciences*, *21*(5), 1805.
6. Shao, L. R., Habela, C. W., & Stafstrom, C. E. (2019). Pediatric epilepsy mechanisms: expanding the paradigm of excitation/inhibition imbalance. *Children*, *6*(2), 23.
7. Sánchez-Villalobos, J. M., Aledo-Serrano, Á., Villegas-Martínez, I., Shaikh, M. F., & Alcaraz, M. (2022). Epilepsy treatment in neuro-oncology: A rationale for drug choice in common clinical scenarios. *Frontiers in Pharmacology*, *13*, 991244.
8. Perucca, E., French, J., & Bialer, M. (2007). Development of new antiepileptic drugs: challenges, incentives, and recent advances. *The lancet neurology*, *6*(9), 793-804.
9. Allen, N. J., & Barres, B. A. (2009). Glia—more than just brain glue. *Nature*, *457*(7230), 675-677.
10. Victor, T. R., & Tsirka, S. E. (2020). Microglial contributions to aberrant neurogenesis and pathophysiology of epilepsy. *Neuroimmunology and neuroinflammation*, *7*, 234.
11. Cho, I. H., Hong, J., Suh, E. C., Kim, J. H., Lee, H., Lee, J. E., ... & Lee, S. J. (2008). Role of microglial IKK $\beta$  in kainic acid-induced hippocampal neuronal cell death. *Brain*, *131*(11), 3019-3033.
12. Hong, J., Cho, I. H., Kwak, K. I., Suh, E. C., Seo, J., Min, H. J., ... & Lee, S. J. (2010). Microglial Toll-like receptor 2 contributes to kainic acid-induced glial activation and hippocampal neuronal cell death. *Journal of biological chemistry*, *285*(50), 39447-39457.
13. Vezzani, A., Ravizza, T., Bedner, P., Aronica, E., Steinhäuser, C., & Boison, D. (2022). Astrocytes in the initiation and progression of epilepsy. *Nature Reviews*

*Neurology*, 18(12), 707-722.

14. Pandit, S., Neupane, C., Woo, J., Sharma, R., Nam, M. H., Lee, G. S., ... & Park, J. B. (2020). Bestrophen1-mediated tonic GABA release from reactive astrocytes prevents the development of seizure-prone network in kainate-injected hippocampi. *Glia*, 68(5), 1065-1080.
15. Álvarez-Ferradas, C., Morales, J. C., Wellmann, M., Nualart, F., Roncagliolo, M., Fuenzalida, M., & Bonansco, C. (2015). Enhanced astroglial Ca<sup>2+</sup> signaling increases excitatory synaptic strength in the epileptic brain. *Glia*, 63(9), 1507-1521.
16. Sano, F., Shigetomi, E., Shinozaki, Y., Tsuzuki-yama, H., Saito, K., Mikoshiba, K., ... & Koizumi, S. (2021). Reactive astrocyte-driven epileptogenesis is induced by microglia initially activated following status epilepticus. *JCI insight*, 6(9).
17. Kinoshita, S., & Koyama, R. (2021). Pro-and anti-epileptic roles of microglia. *Neural regeneration research*, 16(7), 1369-1371.
18. Hiragi, T., Ikegaya, Y., & Koyama, R. (2018). Microglia after seizures and in epilepsy. *Cells*, 7(4), 26.
19. Eyo, U. B., Peng, J., Swiatkowski, P., Mukherjee, A., Bispo, A., & Wu, L. J. (2014). Neuronal hyperactivity recruits microglial processes via neuronal NMDA receptors and microglial P2Y<sub>12</sub> receptors after status epilepticus. *Journal of Neuroscience*, 34(32), 10528-10540.
20. Wu, W., Li, Y., Wei, Y., Bosco, D. B., Xie, M., Zhao, M. G., ... & Wu, L. J. (2020). Microglial depletion aggravates the severity of acute and chronic seizures in mice. *Brain, behavior, and immunity*, 89, 245-255.
21. Dheer, A., Bosco, D. B., Zheng, J., Wang, L., Zhao, S., Haruwaka, K., ... & Wu, L. J. (2024). Chemogenetic approaches reveal dual functions of microglia in seizures. *Brain, behavior, and immunity*, 115, 406-418.
22. Zhao, X., Liao, Y., Morgan, S., Mathur, R., Feustel, P., Mazurkiewicz, J., ... & Huang, Y. (2018). Noninflammatory changes of microglia are sufficient to cause epilepsy. *Cell reports*, 22(8), 2080-2093.
23. Kim, Y. M., & Shin, E. C. (2021). Type I and III interferon responses in SARS-CoV-2 infection. *Experimental & molecular medicine*, 53(5), 750-760.
24. Kopitar-Jerala, N. (2017). The role of interferons in inflammation and inflammasome activation. *Frontiers in immunology*, 8, 263291.
25. Benveniste, E. N., & Qin, H. (2007). Type I interferons as anti-inflammatory mediators. *Science's STKE*, 2007(416), pe70-pe70.
26. Mazewski, C., Perez, R. E., Fish, E. N., & Platanius, L. C. (2020). Type I interferon (IFN)-regulated activation of canonical and non-canonical signaling pathways. *Frontiers in*

*immunology*, 11, 606456.

27. Stanifer, M. L., Pervolaraki, K., & Boulant, S. (2019). Differential regulation of type I and type III interferon signaling. *International journal of molecular sciences*, 20(6), 1445.
28. Goldmann, T., Blank, T., & Prinz, M. (2016). Fine-tuning of type I IFN-signaling in microglia—implications for homeostasis, CNS autoimmunity and interferonopathies. *Current opinion in neurobiology*, 36, 38-42.
29. Blank, T., & Prinz, M. (2017). Type I interferon pathway in CNS homeostasis and neurological disorders. *Glia*, 65(9), 1397-1406.
30. Prudente, A. S., Lee, S. H., Roh, J., Luckemeyer, D. D., Cohen, C. F., Pertin, M., ... & Berta, T. (2024). Microglial STING activation alleviates nerve injury-induced neuropathic pain in male but not female mice. *Brain, Behavior, and Immunity*, 117, 51-65.
31. Donnelly, C. R., Jiang, C., Andriessen, A. S., Wang, K., Wang, Z., Ding, H., ... & Ji, R. R. (2021). STING controls nociception via type I interferon signalling in sensory neurons. *Nature*, 591(7849), 275-280.
32. Hosseini, S., Michaelsen-Preusse, K., Grigoryan, G., Chhatbar, C., Kalinke, U., & Korte, M. (2020). Type I interferon receptor signaling in astrocytes regulates hippocampal synaptic plasticity and cognitive function of the healthy CNS. *Cell Reports*, 31(7).
33. Escoubas, C. C., Dorman, L. C., Nguyen, P. T., Lagares-Linares, C., Nakajo, H., Anderson, S. R., ... & Molofsky, A. V. (2024). Type-I-interferon-responsive microglia shape cortical development and behavior. *Cell*, 187(8), 1936-1954.
34. Viengkhou, B., & Hofer, M. J. (2023). Breaking down the cellular responses to type I interferon neurotoxicity in the brain. *Frontiers in Immunology*, 14, 1110593.
35. Roy, E., & Cao, W. (2022). Glial interference: impact of type I interferon in neurodegenerative diseases. *Molecular Neurodegeneration*, 17(1), 78.
36. Goldmann, T., Zeller, N., Raasch, J., Kierdorf, K., Frenzel, K., Ketscher, L., ... & Prinz, M. (2015). USP 18 lack in microglia causes destructive interferonopathy of the mouse brain. *The EMBO journal*, 34(12), 1612-1629.
37. Raison, C. L., Borisov, A. S., Majer, M., Drake, D. F., Pagnoni, G., Woolwine, B. J., ... & Miller, A. H. (2009). Activation of central nervous system inflammatory pathways by interferon-alpha: relationship to monoamines and depression. *Biological psychiatry*, 65(4), 296-303.
38. Jin, M., Xu, R., Wang, L., Alam, M. M., Ma, Z., Zhu, S., ... & Jiang, P. (2022). Type-I-interferon signaling drives microglial dysfunction and senescence in human iPSC models of Down syndrome and Alzheimer's disease. *Cell Stem Cell*, 29(7), 1135-1153.
39. Udeochu, J. C., Amin, S., Huang, Y., Fan, L., Torres, E. R. S., Carling, G. K., ... & Gan, L. (2023). Tau activation of microglial cGAS-IFN reduces MEF2C-mediated cognitive

resilience. *Nature neuroscience*, 26(5), 737-750.

40. Bialas, A. R., Presumey, J., Das, A., van der Poel, C. E., Lapchak, P. H., Mesin, L., ... & Carroll, M. C. (2017). Microglia-dependent synapse loss in type I interferon-mediated lupus. *Nature*, 546(7659), 539-543.
41. Roy, E. R., Chiu, G., Li, S., Propson, N. E., Kanchi, R., Wang, B., ... & Cao, W. (2022). Concerted type I interferon signaling in microglia and neural cells promotes memory impairment associated with amyloid  $\beta$  plaques. *Immunity*, 55(5), 879-894.
42. Ejlerskov, P., Hultberg, J. G., Wang, J., Carlsson, R., Ambjørn, M., Kuss, M., ... & Issazadeh-Navikas, S. (2015). Lack of neuronal IFN- $\beta$ -IFNAR causes Lewy body-and Parkinson's disease-like dementia. *Cell*, 163(2), 324-339.
43. Bosco, D. B., Zheng, J., Xu, Z., Peng, J., Eyo, U. B., Tang, K., ... & Wu, L. J. (2018). RNAseq analysis of hippocampal microglia after kainic acid-induced seizures. *Molecular brain*, 11, 1-13.
44. Shakil, A. O., Di Bisceglie, A. M., & Hoofnagle, J. H. (1996). Seizures during alpha interferon therapy. *Journal of hepatology*, 24(1), 48-51.
45. Pavlovsky\*, L., Seiffert\*, E., Heinemann, U., Korn, A., Golan, H., & Friedman, A. (2005). Persistent BBB disruption may underlie alpha interferon-induced seizures. *Journal of neurology*, 252, 42-46.
46. Kostoula, C., Shaker, T., Cerovic, M., Craparotta, I., Marchini, S., Butti, E., ... & Vezzani, A. (2019). TLR3 preconditioning induces anti-inflammatory and anti-ictogenic effects in mice mediated by the IRF3/IFN- $\beta$  axis. *Brain, behavior, and immunity*, 81, 598-607.
47. Racine, R. J. (1972). Modification of seizure activity by electrical stimulation: II. Motor seizure. *Electroencephalography and clinical neurophysiology*, 32(3), 281-294.
48. Rusina, E., Bernard, C., & Williamson, A. (2021). The kainic acid models of temporal lobe epilepsy. *Eneuro*, 8(2).
49. Cerri, C., Genovesi, S., Allegra, M., Pistillo, F., Püntener, U., Guglielmotti, A., ... & Caleo, M. (2016). The chemokine CCL2 mediates the seizure-enhancing effects of systemic inflammation. *Journal of Neuroscience*, 36(13), 3777-3788.
50. Griffith, J. L., & Wong, M. (2018). The mTOR pathway in treatment of epilepsy: a clinical update. *Future neurology*, 13(2), 49-58.
51. Zeng, L. H., Rensing, N. R., & Wong, M. (2009). The mammalian target of rapamycin signaling pathway mediates epileptogenesis in a model of temporal lobe epilepsy. *Journal of Neuroscience*, 29(21), 6964-6972.

52. Okoh, J., Mays, J., Bacq, A., Oses-Prieto, J. A., Tyanova, S., Chen, C. J., ... & Costa-Mattioli, M. (2023). Targeted suppression of mTORC2 reduces seizures across models of epilepsy. *Nature Communications*, *14*(1), 7364.
53. Zhao, X., Liao, Y., Morgan, S., Mathur, R., Feustel, P., Mazurkiewicz, J., ... & Huang, Y. (2018). Noninflammatory changes of microglia are sufficient to cause epilepsy. *Cell reports*, *22*(8), 2080-2093.

Abstract in Korean

## Kainic acid 유도 마우스 뇌전증 모델에서 1형 인터페론 신호전달경로의 역할 규명

뇌전증은 신경세포의 과도한 활성화로 인한 반복적인 발작을 특징으로 하는 만성 신경학적 질환이다. 신경세포의 활성을 표적하는 다양한 항뇌전증제가 개발되어 왔지만, 환자들 중 약 30%는 이러한 치료제에 반응하지 않으며, 이는 뇌전증 병리 기전에 대한 더 깊은 이해가 필요함을 의미한다. 제1형 인터페론은 뇌의 발달과 항상성 유지에 중요한 기능을 담당하는 것으로 가능성이 제기되어 왔으며, 인터페론 신호전달의 장애는 알츠하이머 질병을 비롯한 다양한 중추신경계 질환과 관련이 있다. 최근 연구에 따르면, kainic acid 로 발작을 유도했을 때 microglia 에서 제1형 인터페론과 관련된 여러 신호전달경로가 활성화된다는 결과가 보고되었다. 그러나 해당 신호전달경로가 발작에서 어떤 역할을 하는지는 아직 명확히 밝혀지지 않았다. 그렇기에 본 연구에서는 발작 조건에서 인터페론 역할을 규명하고자 하였다. 신경흥분성 아미노산 작용제인 kainic acid 를 마우스에 주사하여 발작을 유도하였고, 발작의 세기와 발작으로 인해 뇌에서 일어나는 여러 반응들을 wild-type 마우스와 제1형 인터페론 수용체가 결손된 *Ifnar1* knockout 마우스에서 비교하였다. 흥미롭게도, *Ifnar1* knockout 마우스에서 발작의 세기가 감소하였으며 발작 초기 단계에서 신경세포의 흥분 감소와 microglia 활성화 차이를 확인할 수 있었다. 이러한 결과는 제1형 인터페론의 발작 및 뇌전증 치료제로서의 잠재력을 가질 수 있음을 시사한다.

---

핵심되는 말 : 뇌전증, 발작, 인터페론, 미세아교세포, 신경세포